The Abdus Salam International Centre for Theoretical Physics

2354-28

**Summer School on Cosmology**

*16 - 27 July 2012*

**Lensing - Lecture 3**

H. Hoekstra
*Leiden Observatory*

Strada Costiera, 11 - 34151 - Trieste - Italy • Tel. +39 0402240111 • Fax +39 040224163 • sci_info@ictp.it • www.ictp.it
ICTP is governed by UNESCO, IAEA and Italy, and it is a UNESCO Category 1 Institute

# WEAK LENSING:

## PRACTICAL CONSIDERATIONS

# Weak lensing is noisy

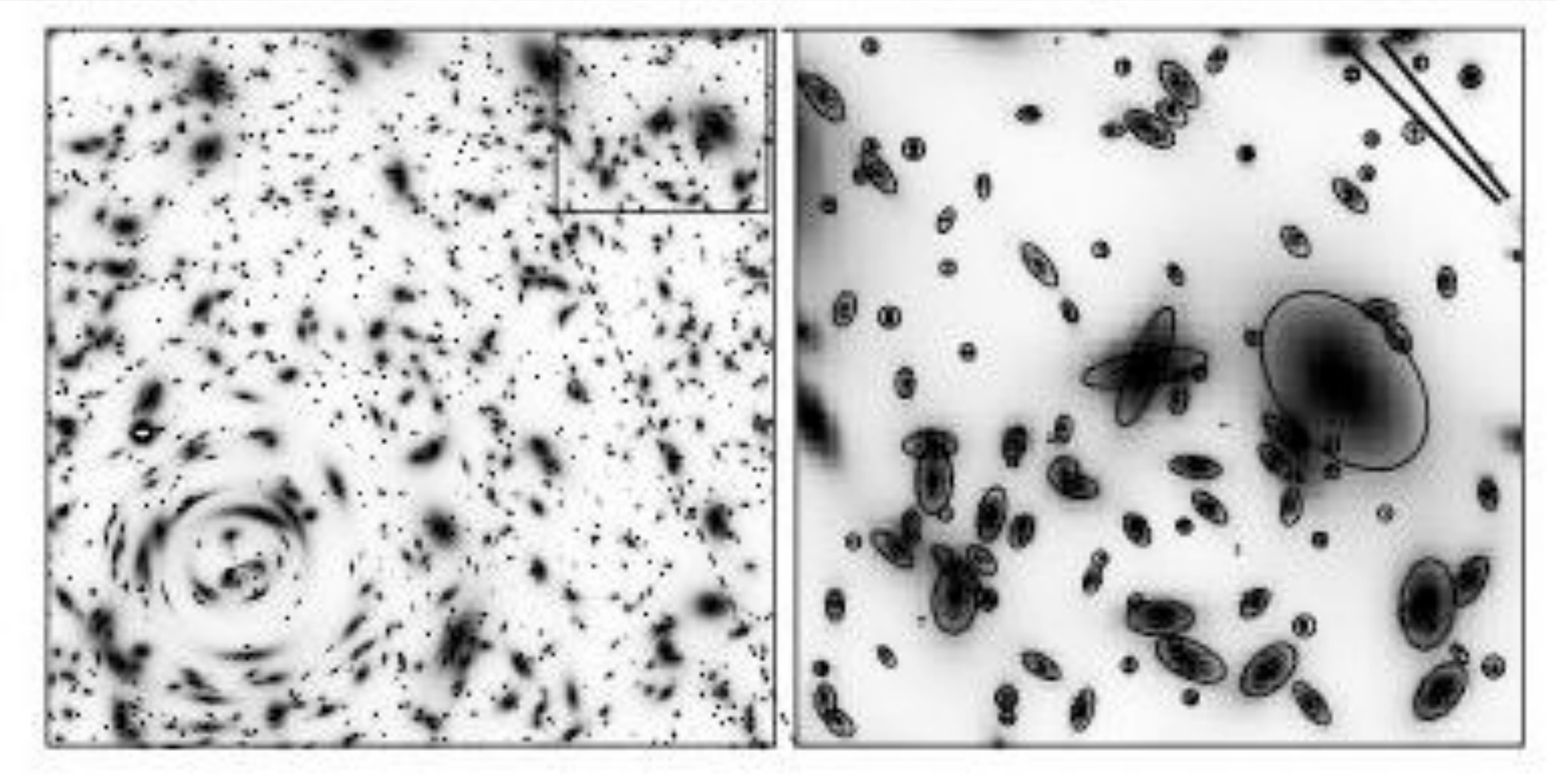

A measurement of the ellipticity of a galaxy provides an unbiased but noisy measurement of the shear.

# Weak lensing is noisy

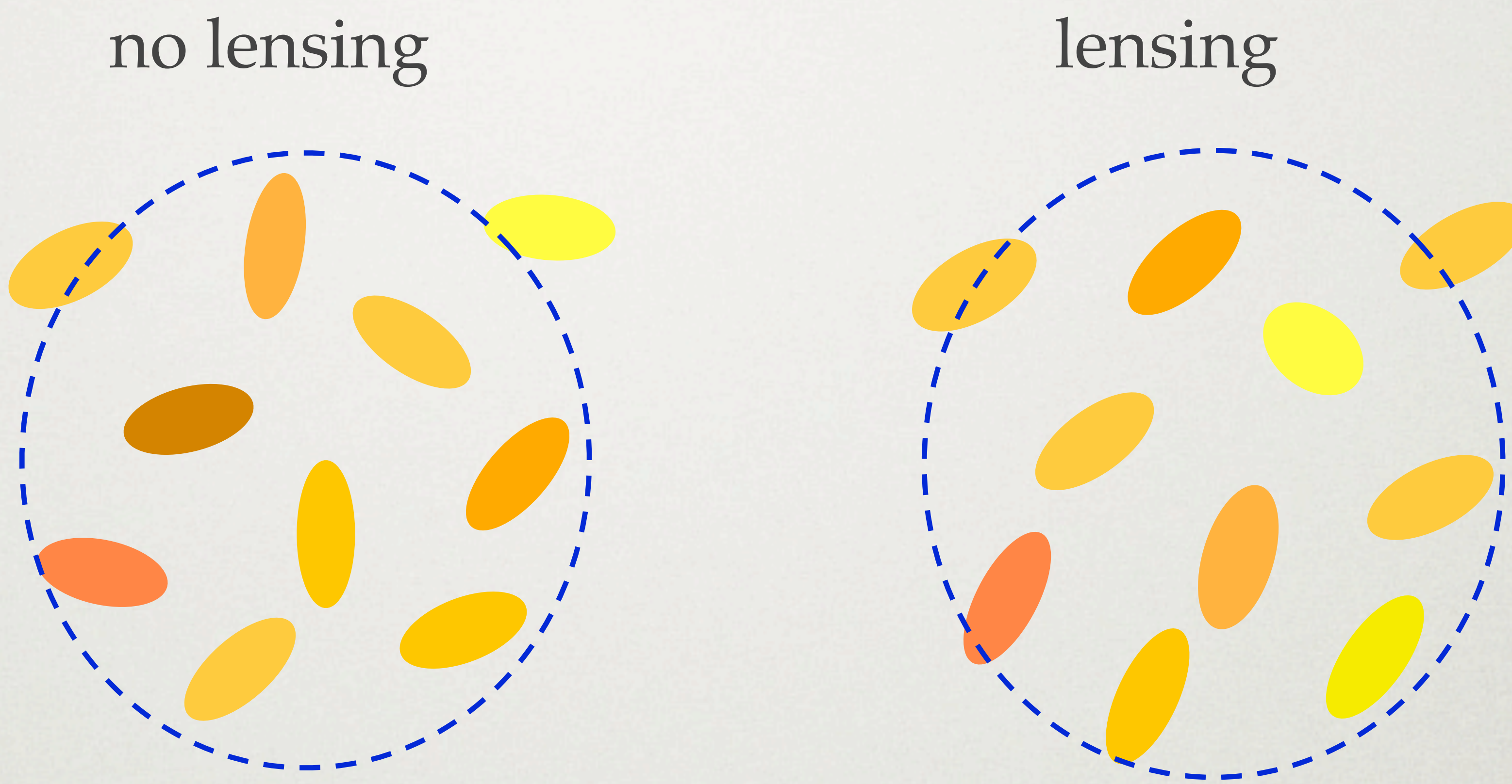


Averaged shape: $\langle e \rangle = 0$ $\langle e \rangle \approx \gamma$

Unlensed galaxies have an intrinsic ellipticity of 0.30, which is much larger than the weak lensing shears we are interested in.

# Precision ≠ Accuracy

For accurate cosmology we need:

**- accurate shapes for the sources**
- accurate photometric redshifts
- accurate interpretation of the signal

- Observational distortions are larger than the signal
- Galaxies are too faint for large spectroscopic surveys
- Sensitive to non-linear structure formation

# Galaxies are small...

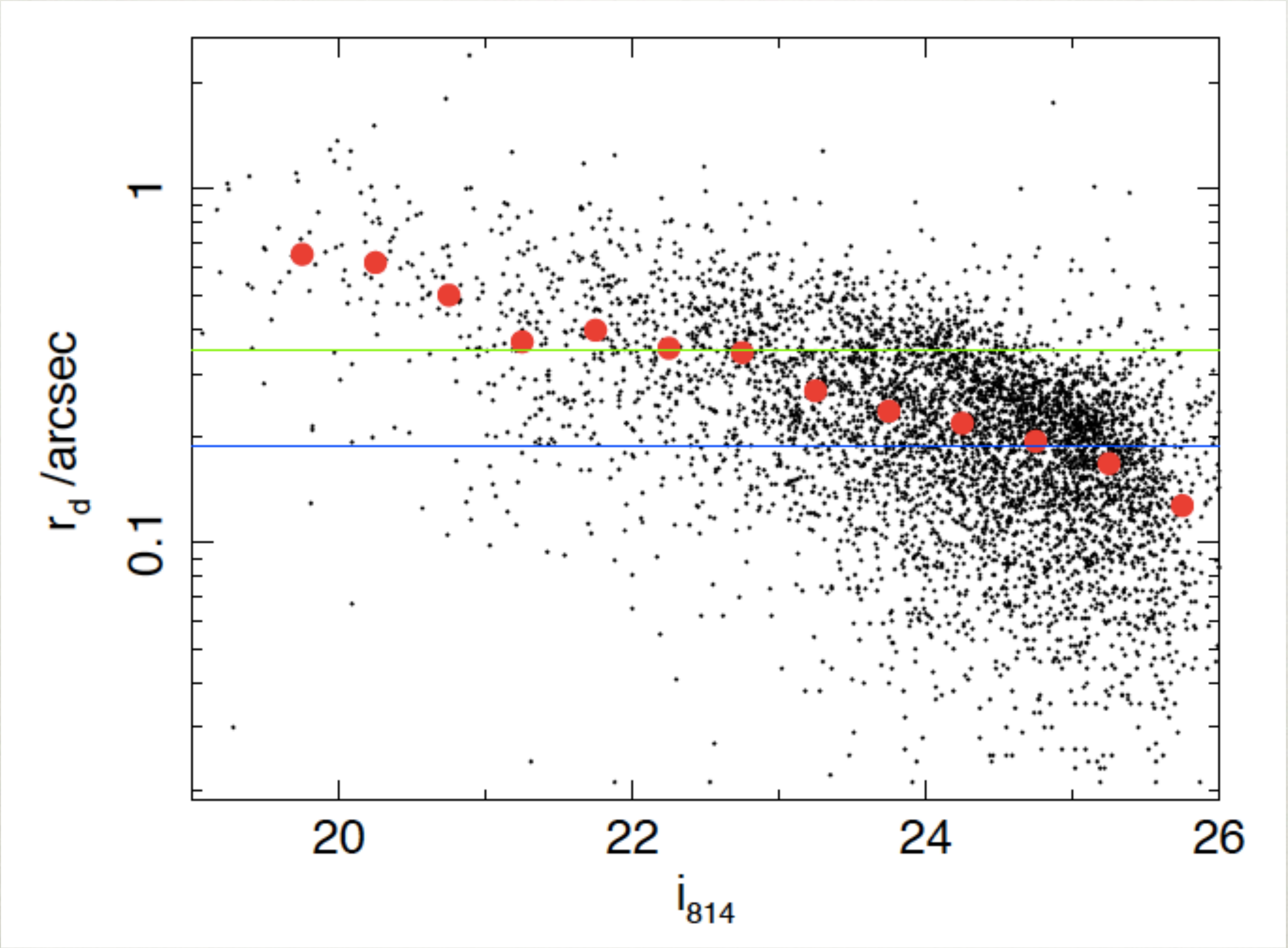


Miller et al. (in prep)

# ... AND FAINT

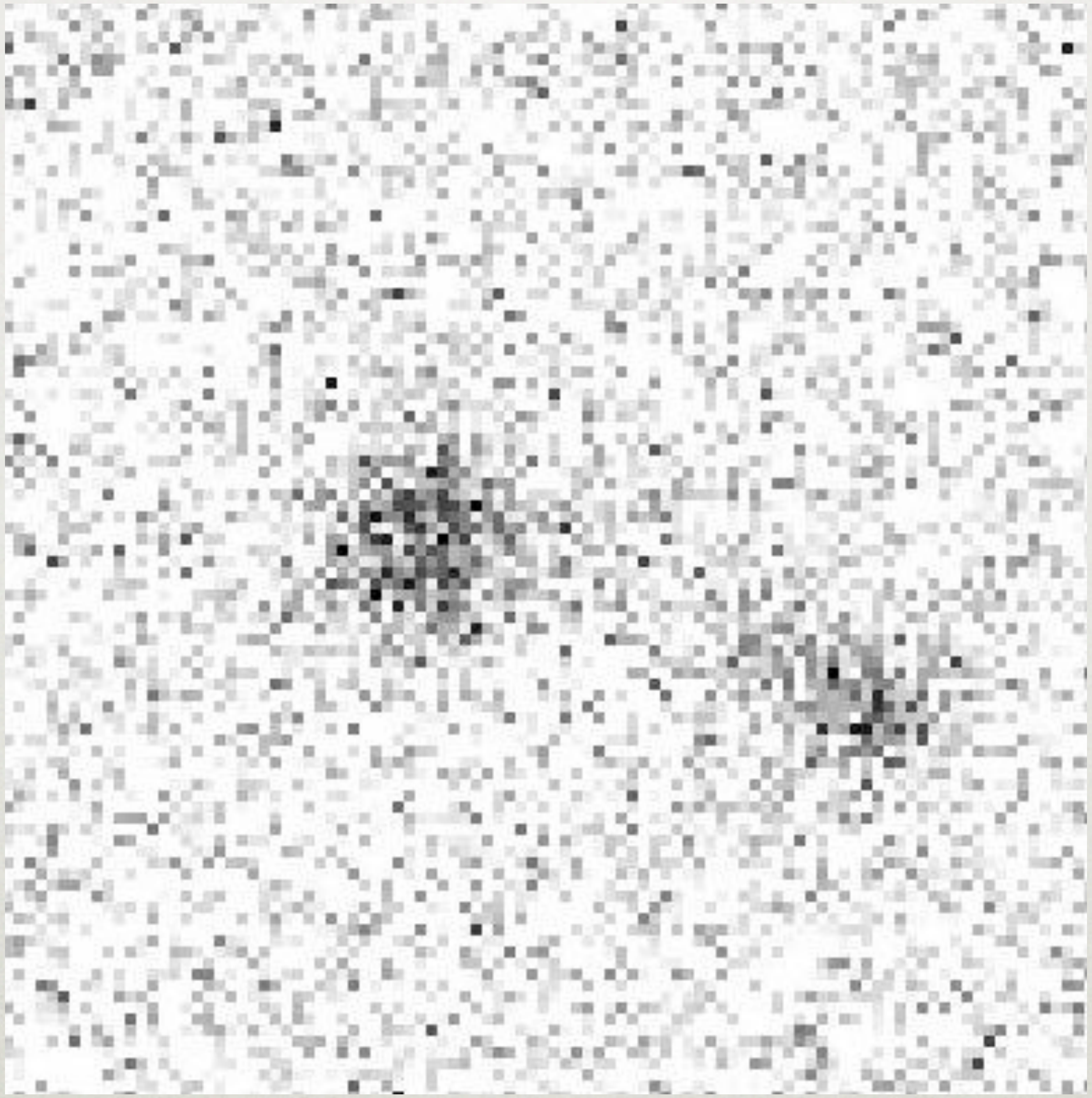

# Quantifying shapes

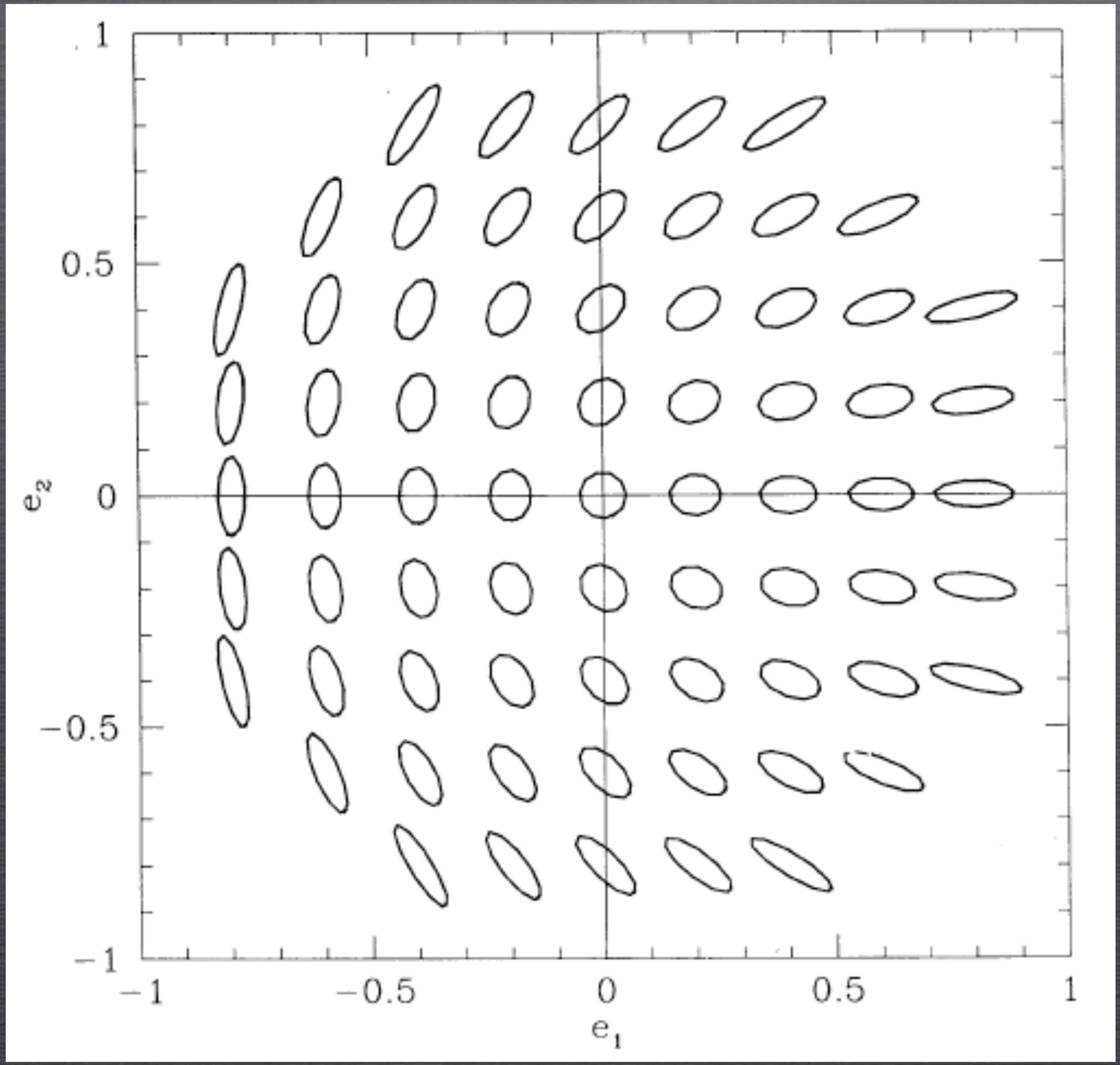


We need two numbers to characterize the shapes

# Quantifying shapes

If we have an object with axis ratios a and b:

Ellipticity: $\varepsilon = 1 - b / a$

Polarisation: $\chi$ or $e = (a^2 - b^2) / (a^2 + b^2)$

Shear/stretch/distortion: $\gamma = (a-b) / (a+b)$

For small $\varepsilon$: $e = \varepsilon$ and $\gamma = \varepsilon/2 = e/2$

These are equivalent, but often called the wrong name

# Quantifying shapes

Shapes can be determined following two fundamentally different approaches.

- parametric (fitting a PSF convolved model)
  *see e.g. Miller et al. (2007) for more information*

- non-parametric (moments)
  *we will focus on these for reasons of simplicity (and lack of time)*

# Unweighted moments

Paulin-Hendriksson et al. (2008)

$$F^{(0)} = \int \mathrm{d}^2\boldsymbol{x}\, f(\boldsymbol{x})$$

Total flux: 0th moment

$$x_i^{\mathrm{cen}} = \frac{F_i^{(1)}}{F^{(0)}} = \frac{1}{F^{(0)}} \int \mathrm{d}^2\boldsymbol{x}\, x_i\, f(\boldsymbol{x})$$

Position: 2nd moment

$$Q_{ij} = \frac{F_{ij}^{(2)}}{F^{(0)}} = \frac{1}{F^{(0)}} \int \mathrm{d}^2\boldsymbol{x}\, (x_i - x_i^{\mathrm{cen}})(x_j - x_j^{\mathrm{cen}})\, f(\boldsymbol{x}).$$

Shape/Size: 4th moment

# Unweighted moments

Size: $R^2 \equiv Q_{11} + Q_{22}$

Shape: $\epsilon_1 \equiv \dfrac{Q_{11} - Q_{22}}{Q_{11} + Q_{22}}, \ \epsilon_2 \equiv \dfrac{2Q_{12}}{Q_{11} + Q_{22}}$

# Quadrupole moments

But the galaxies have been convolved with the PSF. For unweighted moments the correction is "easy":

$$R^2_{\mathrm{obs}} = R^2_{\mathrm{gal}} + R^2_{\mathrm{PSF}}$$

$$\varepsilon_{\mathrm{obs}} = \varepsilon_{\mathrm{gal}} + \frac{R^2_{\mathrm{PSF}}}{R^2_{\mathrm{gal}} + R^2_{\mathrm{PSF}}} (\varepsilon_{\mathrm{PSF}} - \varepsilon_{\mathrm{gal}})$$

The corrected polarization is given by:

$$\varepsilon_{\mathrm{gal}} = \frac{\varepsilon_{\mathrm{obs}} R^2_{\mathrm{obs}} - \varepsilon_{\mathrm{PSF}} R^2_{\mathrm{PSF}}}{R^2_{\mathrm{obs}} - R^2_{\mathrm{PSF}}}$$

# A recipe

- Detect objects
- Measure their shapes
- Determine the PSF model
- Correct the galaxies for the PSF

**Done!**

# Detecting objects

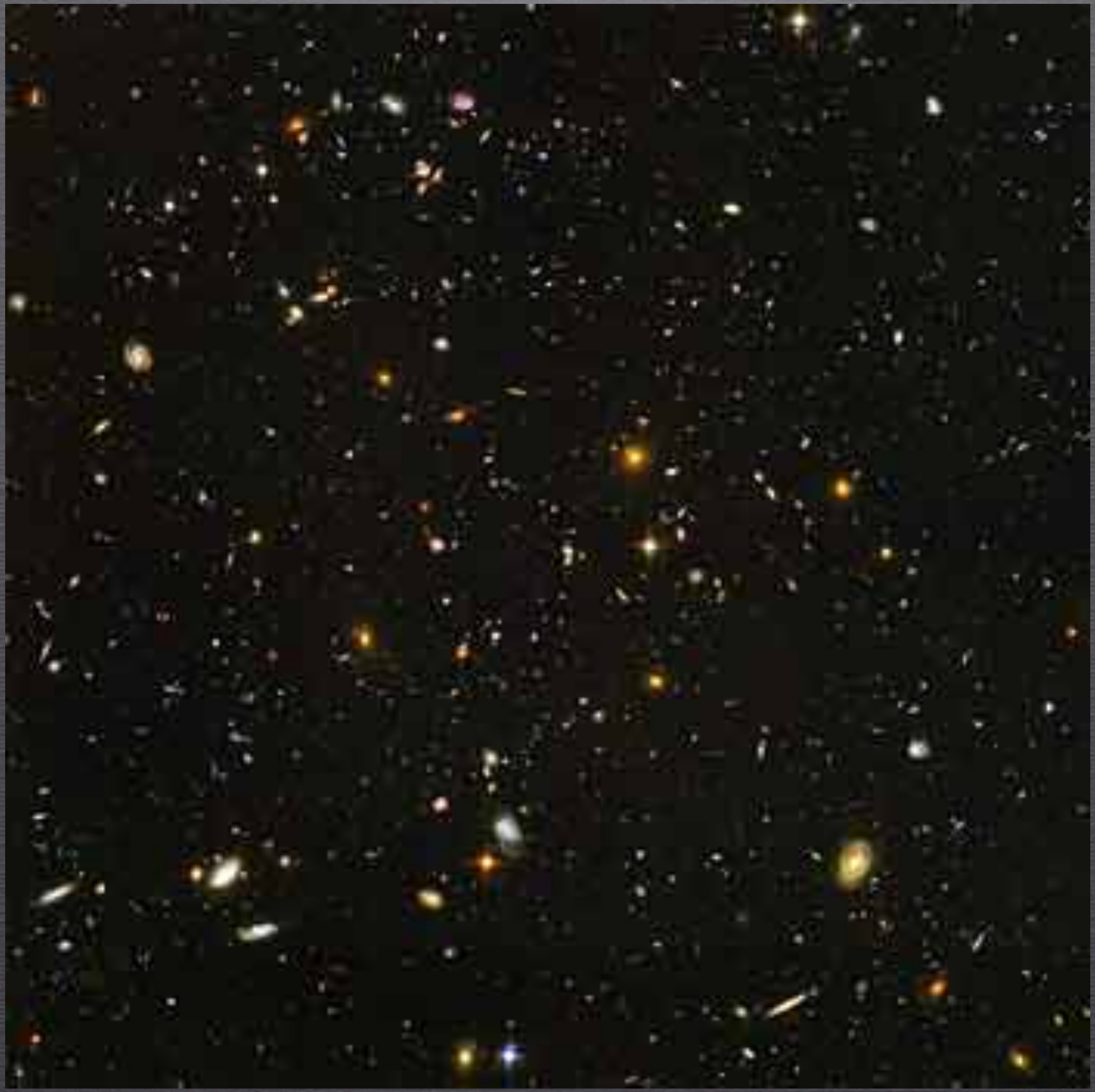

# Detecting objects

A number of "peak finders" exist. The most popular is SExtractor. It is very fast and is versatile.

To find objects in noisy data, one needs to smooth the data with a smoothing kernel. The optimal kernel is a smoothing with the object itself.

A peakfinder that uses a range of smoothing kernels and picks the highest S/N is a hierarchical peak finder.

# Detecting objects

Potential problems:

The smoothing kernel is typically round; this can bias the detection algorithm towards round objects.

Objects may partly overlap; this is called blending. How to define such objects? We would like to avoid using them in a lensing analysis. This problem is more severe for deep, ground-based images.

We need to remove spurious detections (cosmetic defects, diffraction spikes, resolved galaxies)

# Complications

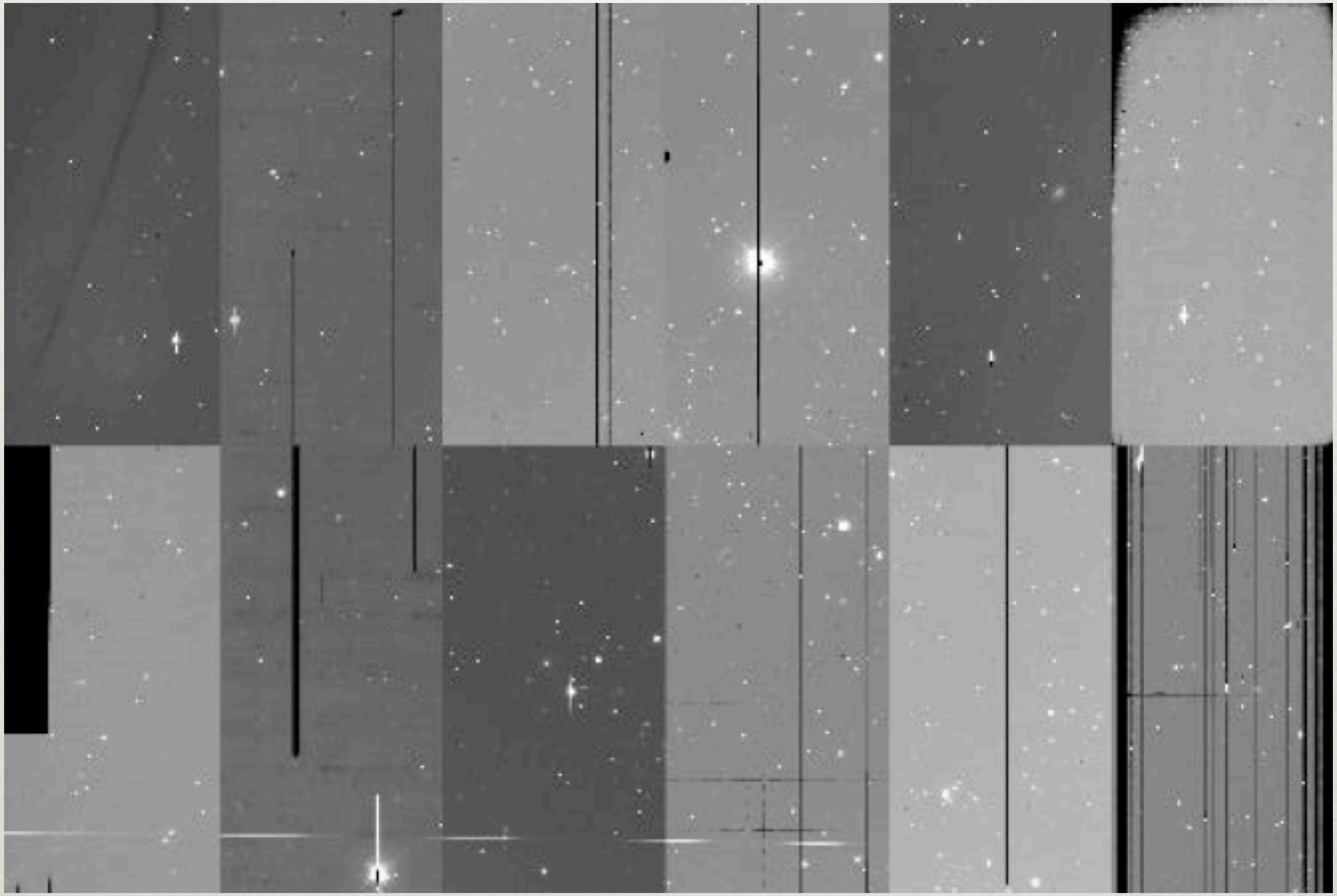

A cfh12k image: real images do not provide uniform coverage of the sky...

# Complications

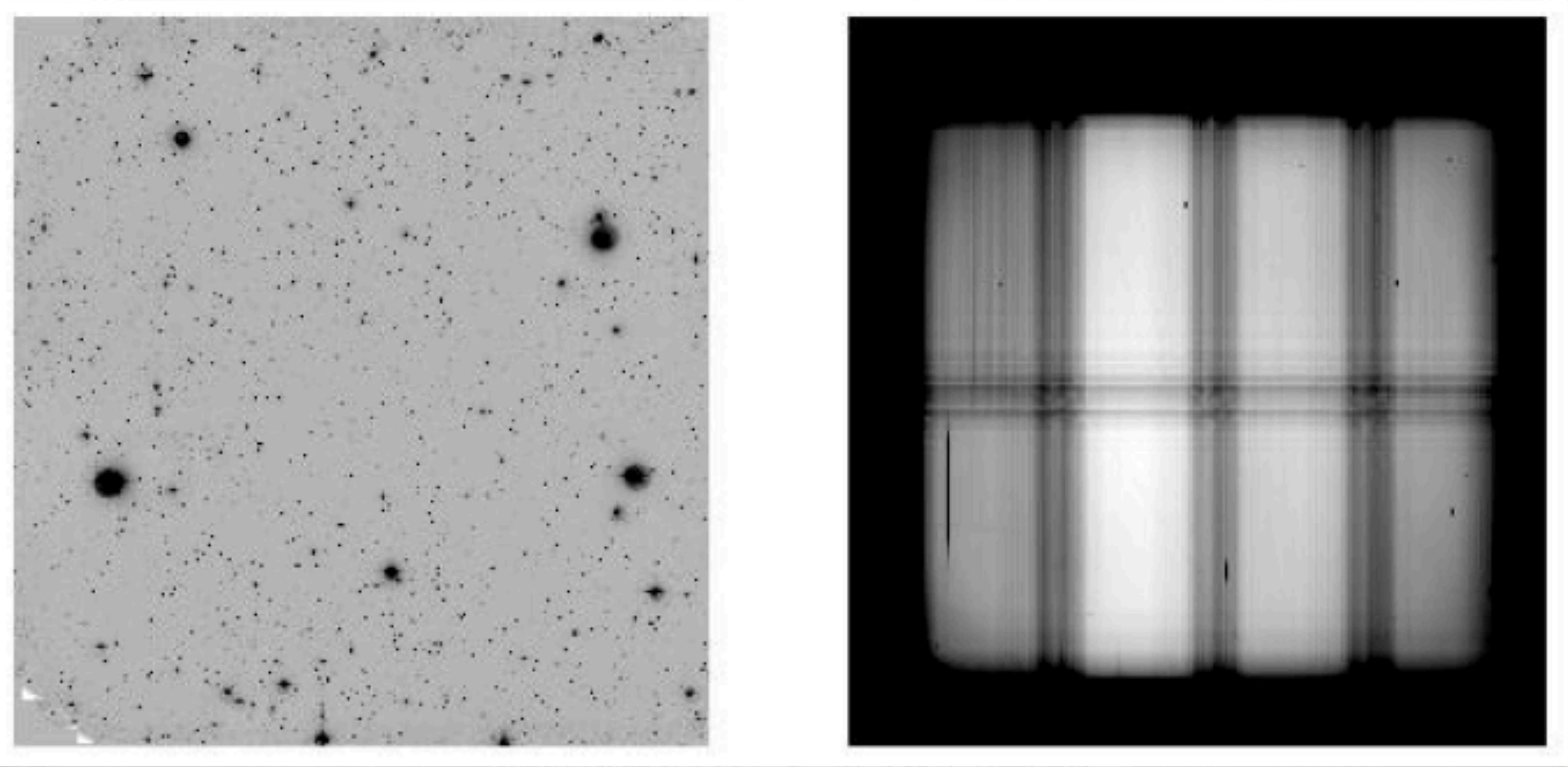

Stack of WFI exposures: have to account for non-uniform coverage. This also complicates dealing with the PSF.

# Measuring shapes

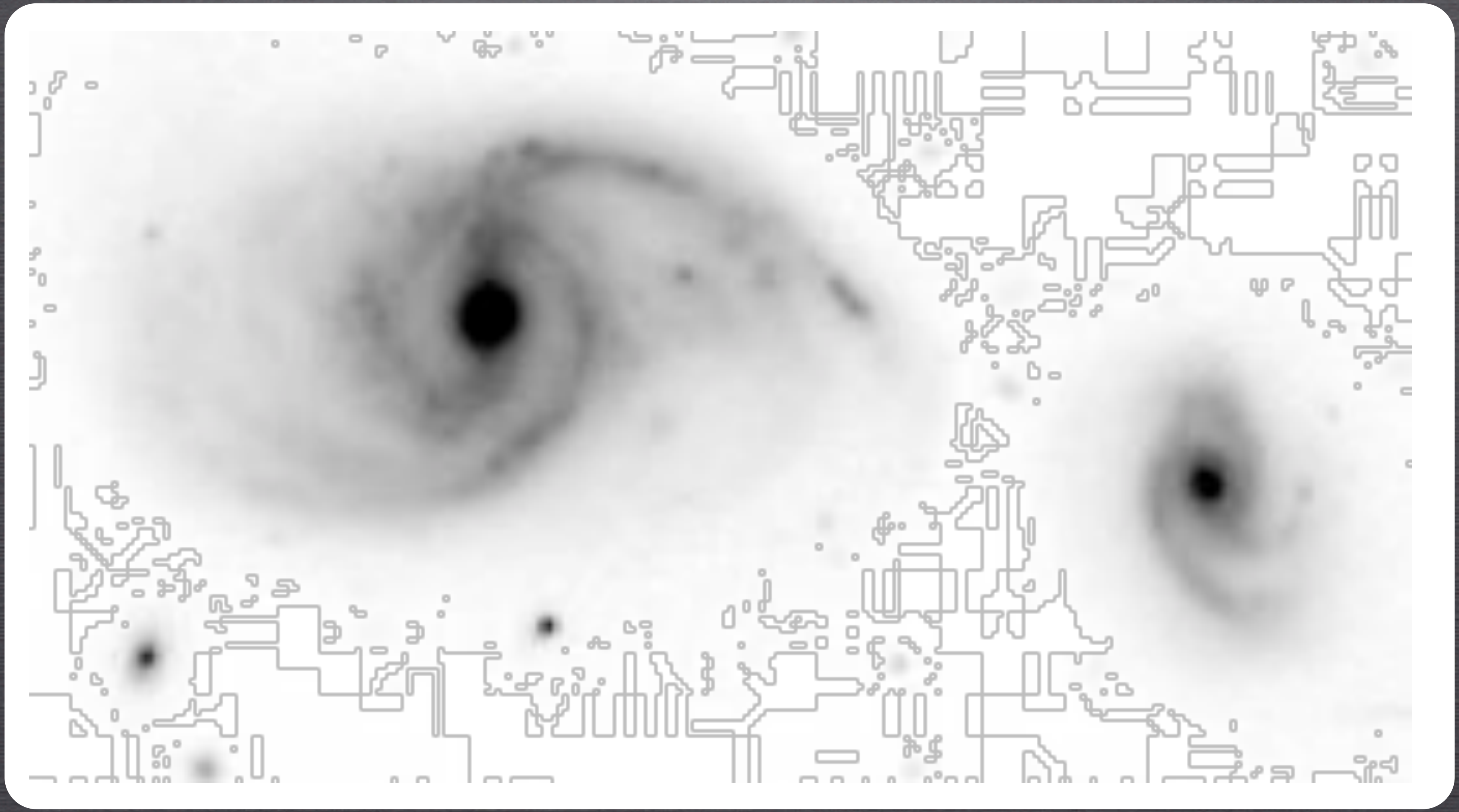

Having found the objects, we now need to quantify their shapes.

# Measuring shapes

Quantifying the shapes of well resolved galaxies is fairly straightforward, but typical weak lensing studies use distant, faint galaxies.

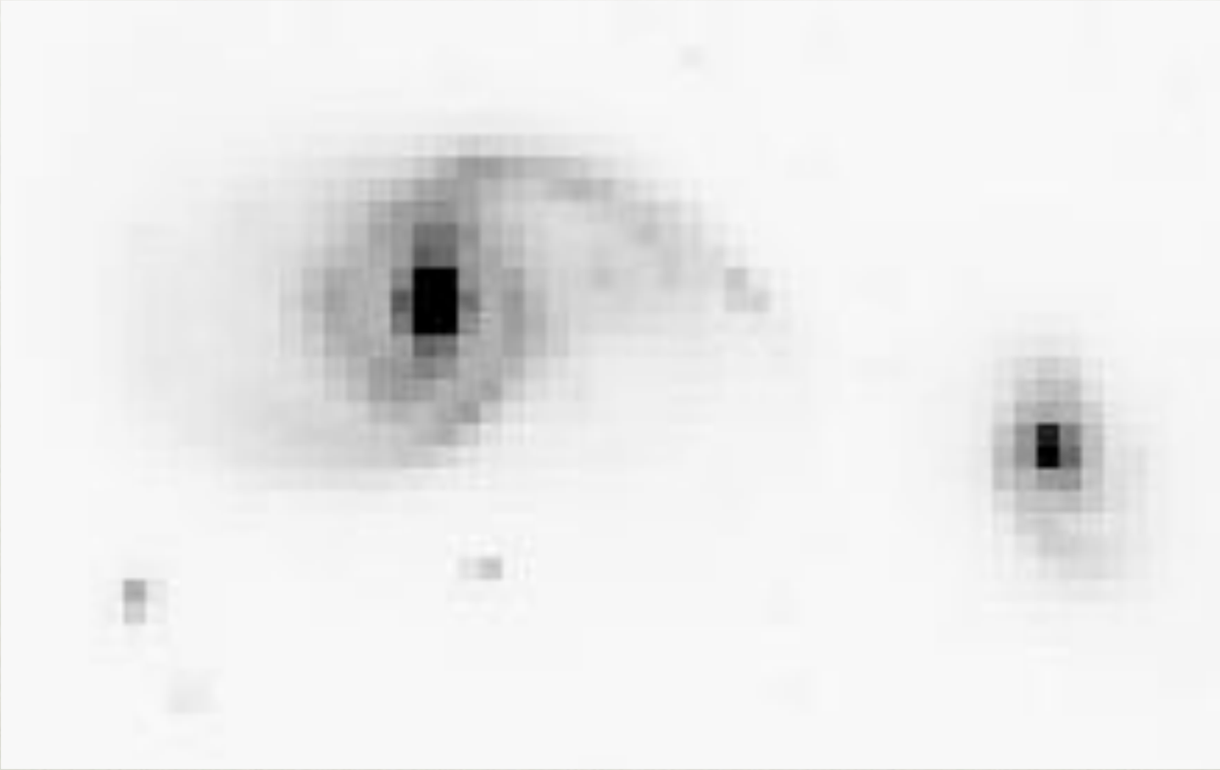

Sampling can become a problem…

# Measuring shapes

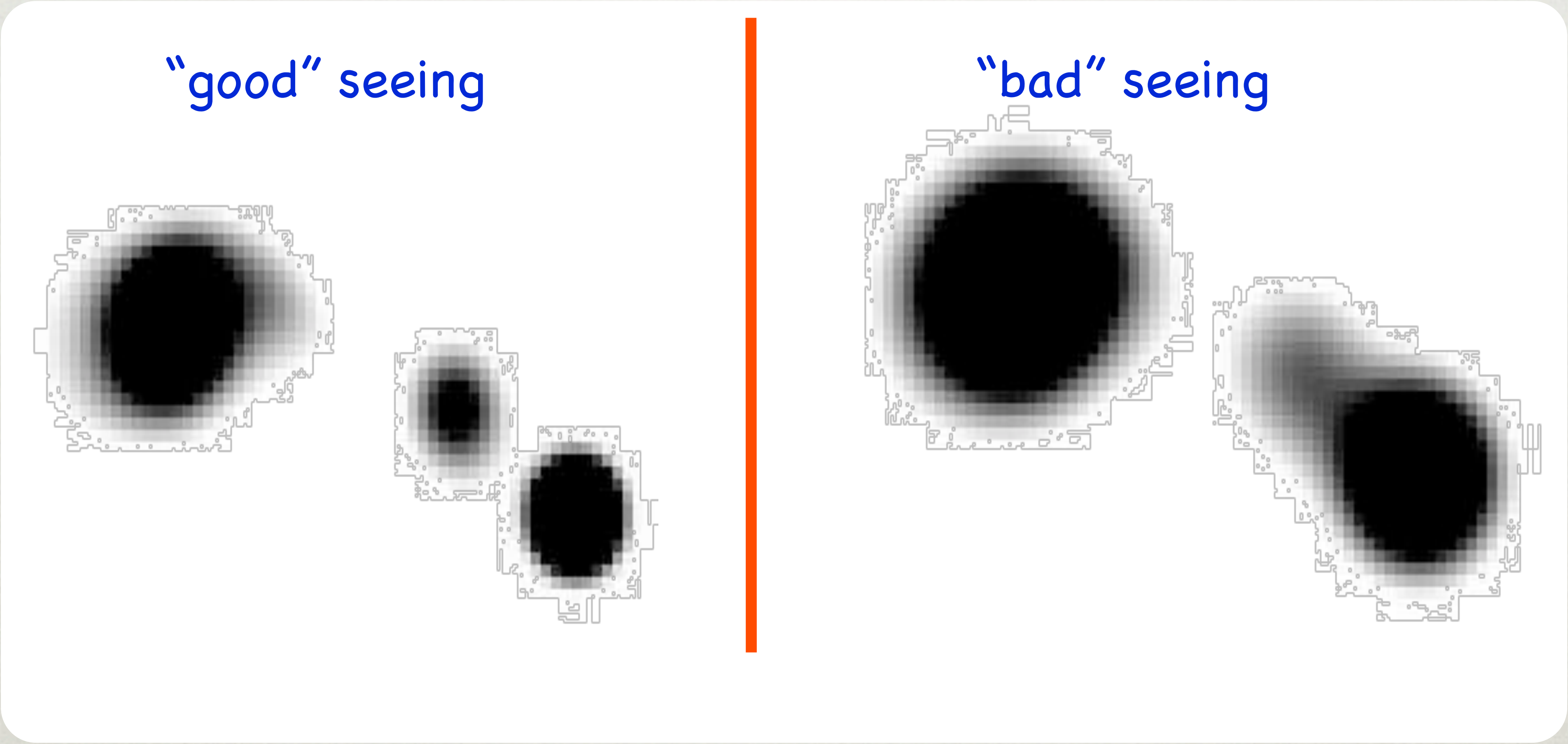


The blurring by the atmosphere is a serious complication

# Measuring shapes

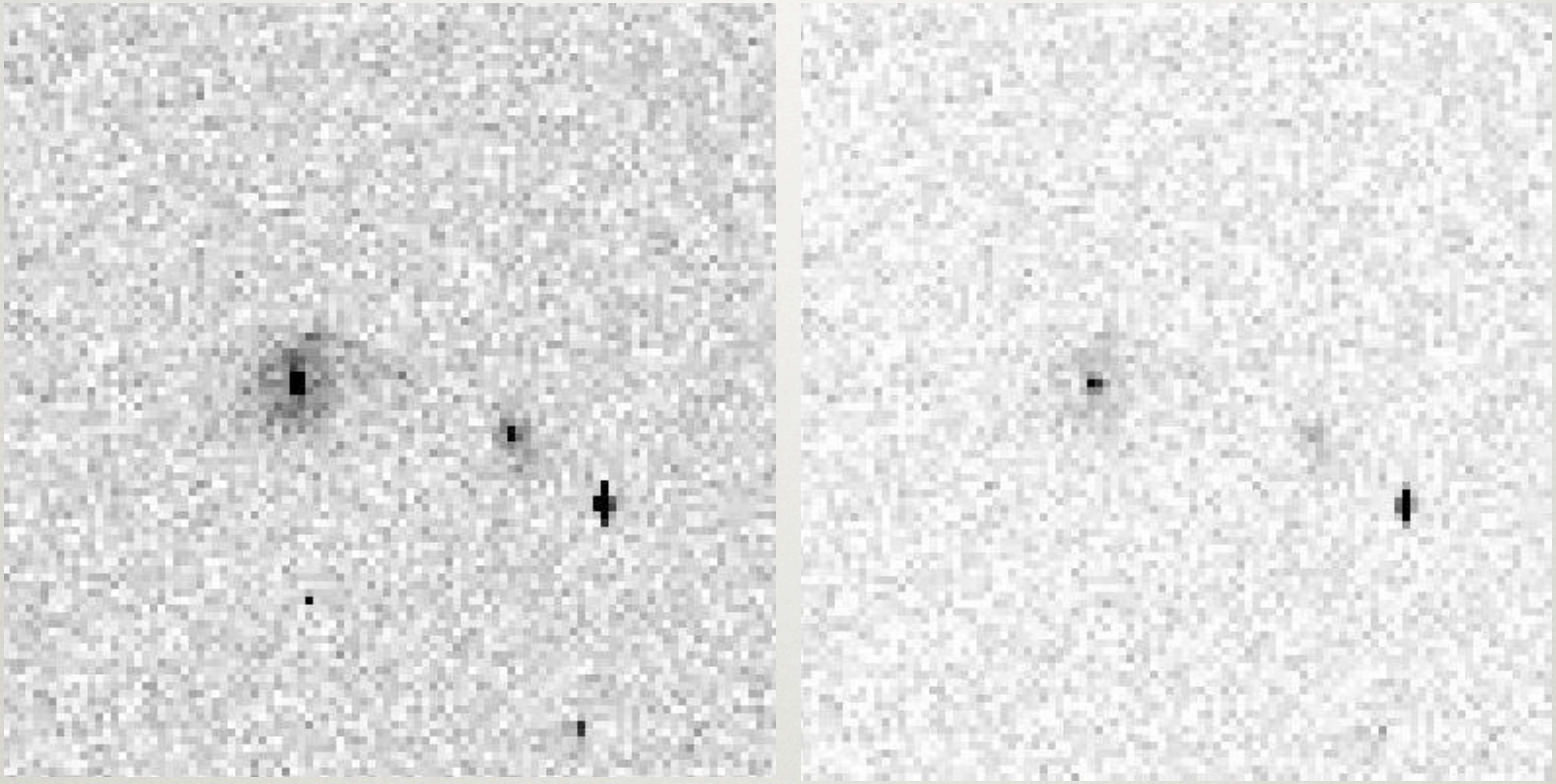

… and then there is noise!

# Measuring shapes

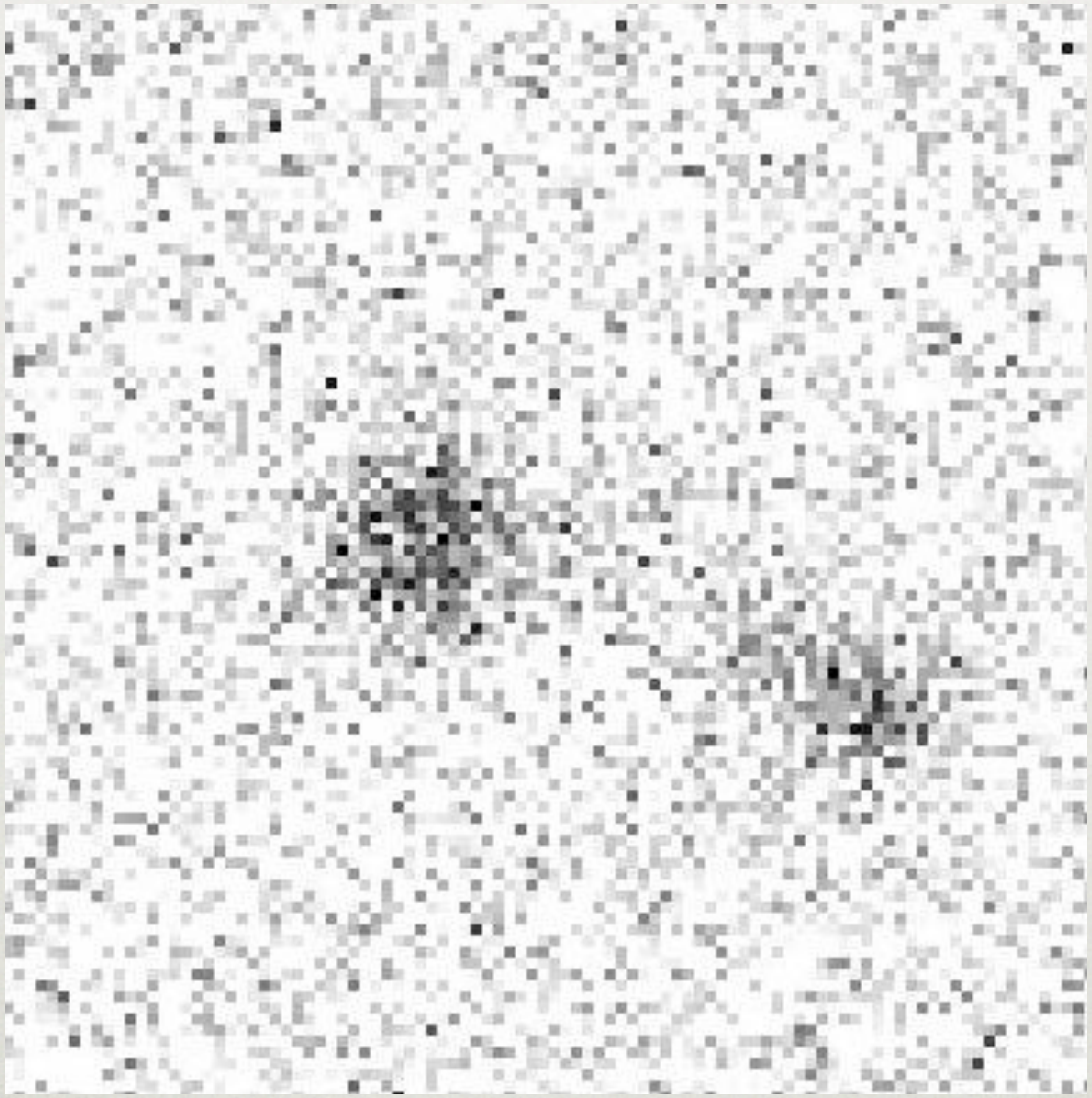

Noise and seeing is a very bad combination!

# Measuring shapes

How can we relate the shape of this…

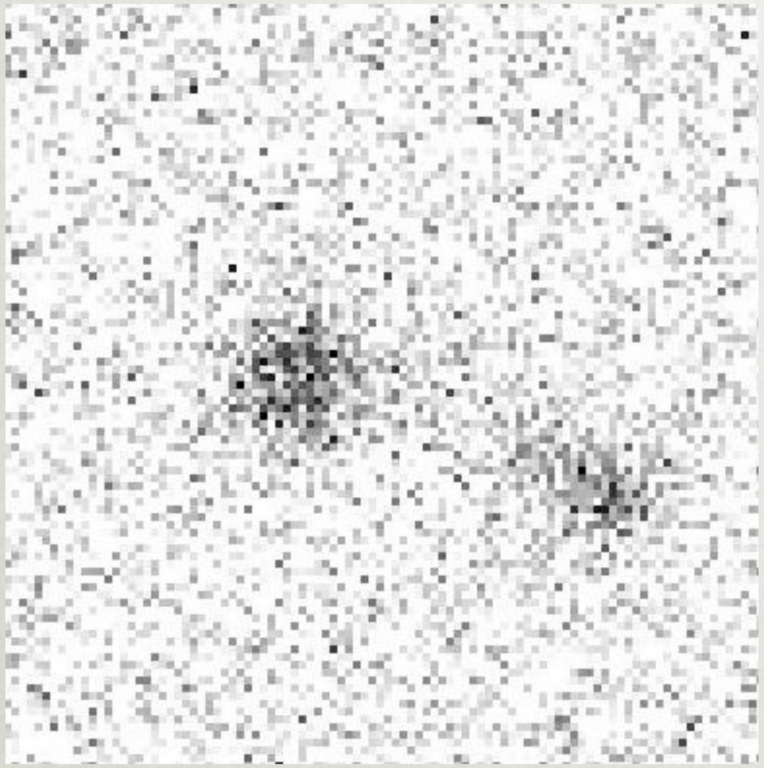

… to this?

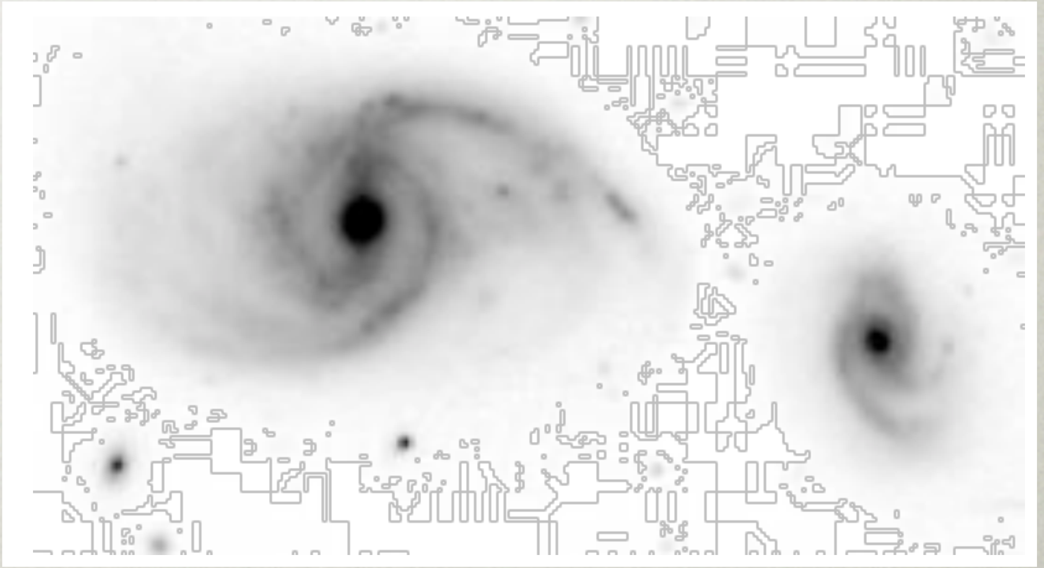

# Measuring shapes

Clearly it becomes harder to measure shapes if

- *The galaxy is faint*
- *The seeing is large (relative to the galaxy size)*

We can only use galaxies that have sizes larger than the size of the PSF. But how much larger?

# Useful galaxies

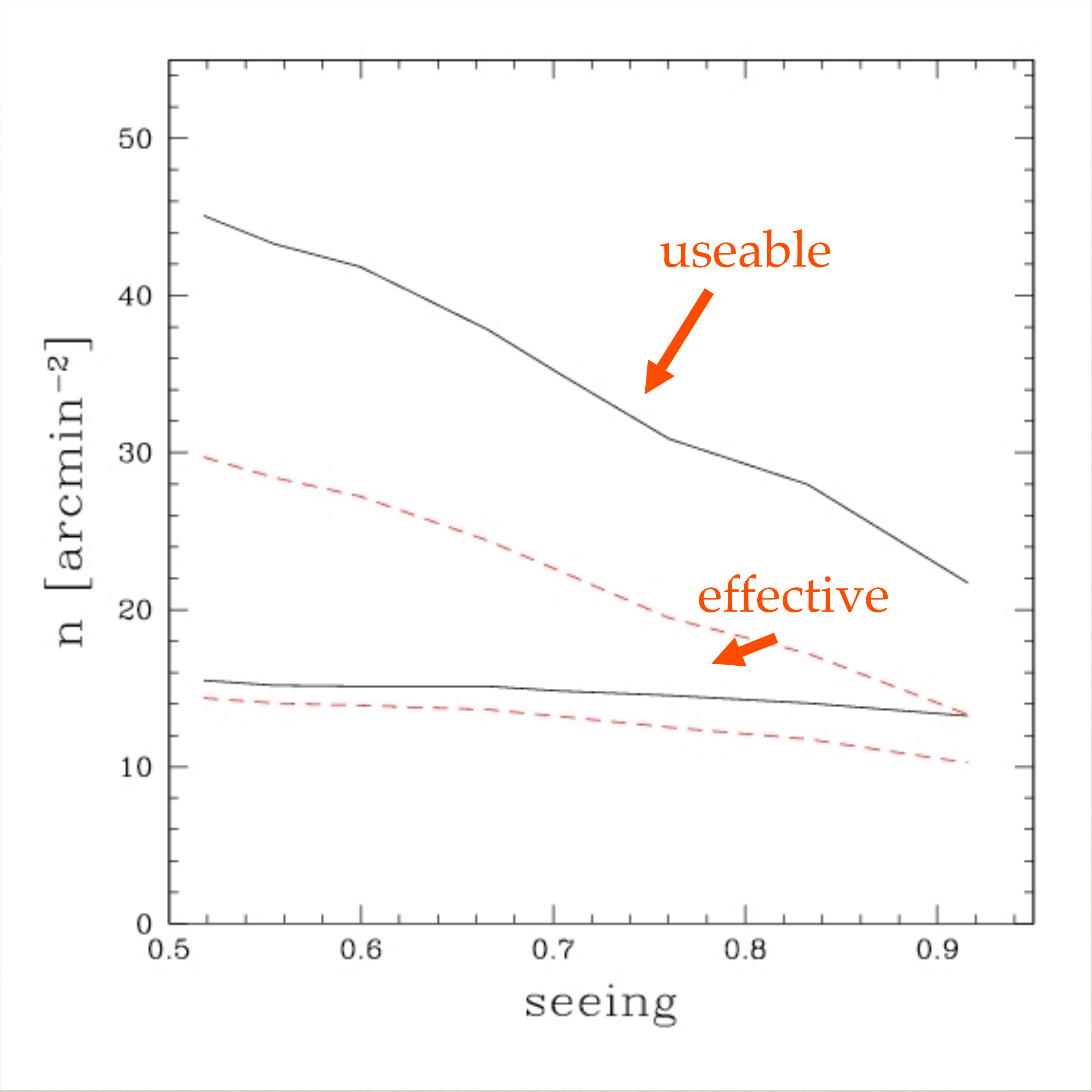

# Useful galaxies

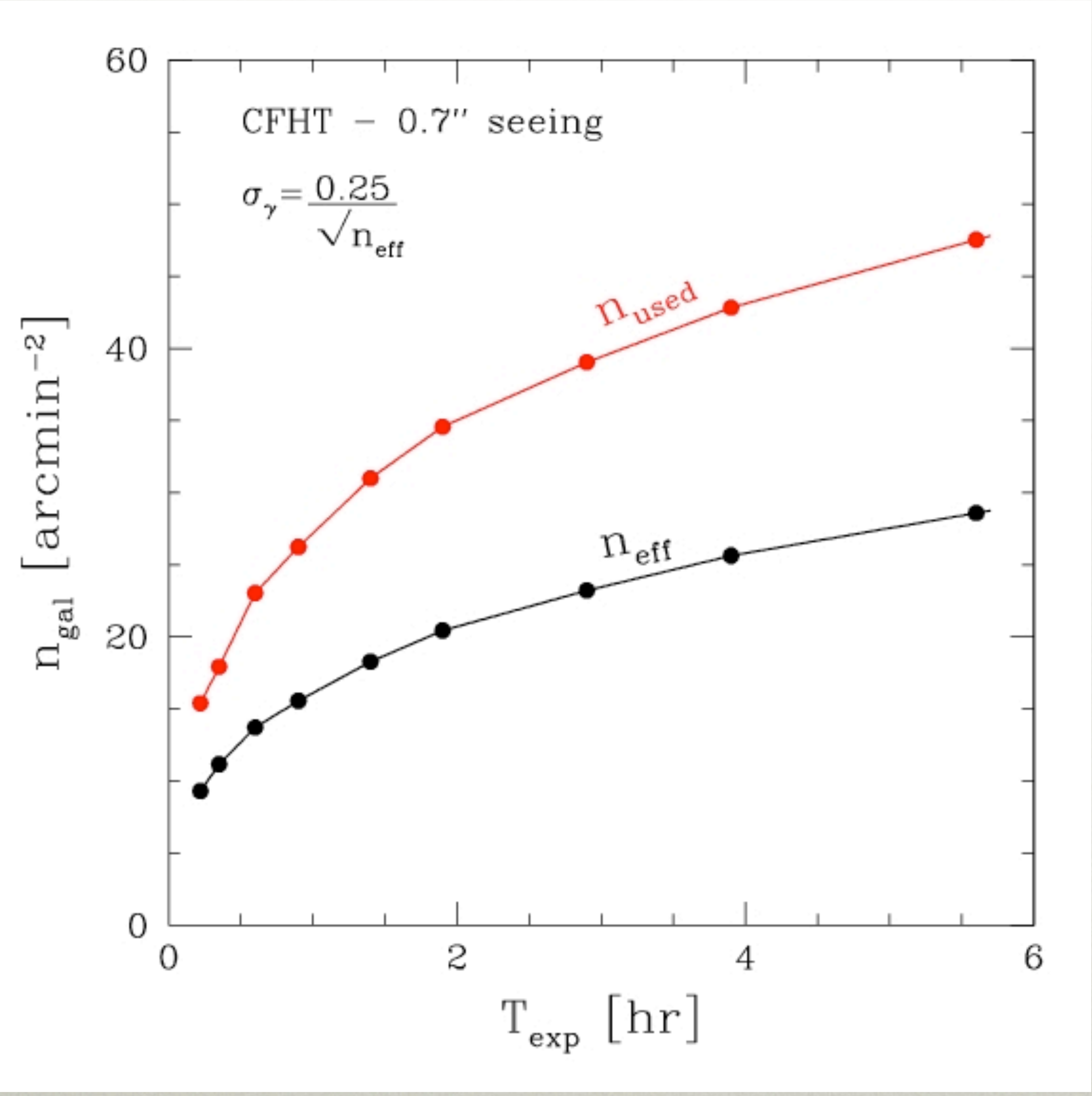


We should use "effective" source densities when computing the expected precision of a survey.

# Correcting the PSF

There are two concerns with PSF correction:

- **is the model for the PSF correct?**
- is the correction itself adequate?

# Correcting the PSF

$$\widehat{\varepsilon_{\rm gal}} \approx \varepsilon_{\rm gal} + \frac{\partial \varepsilon_{\rm gal}}{\partial (R^2_{\rm PSF})}\delta(R^2_{\rm PSF}) + \frac{\partial \varepsilon_{\rm gal}}{\partial \varepsilon_{\rm PSF}}\delta\varepsilon_{\rm PSF}$$

$$\frac{\partial \varepsilon_{\rm gal}}{\partial (R^2_{\rm PSF})} = \frac{R^2_{\rm obs}}{R^2_{\rm obs} - R^2_{\rm PSF}}(\varepsilon_{\rm obs} - \varepsilon_{\rm PSF}) = \frac{\varepsilon_{\rm gal} - \varepsilon_{\rm PSF}}{R^2_{\rm gal}}$$

$$\frac{\partial \varepsilon_{\rm gal}}{\partial \varepsilon_{\rm PSF}} = -\frac{R^2_{\rm PSF}}{R^2_{\rm obs} - R^2_{\rm PSF}} = -\frac{R^2_{\rm PSF}}{R^2_{\rm gal}} \; .$$

$$\widehat{\varepsilon_{\rm gal}} \approx \left\{1 + \frac{\delta(R^2_{\rm PSF})}{R^2_{\rm gal}}\right\}\varepsilon_{\rm gal} - \left\{\frac{R^2_{\rm PSF}}{R^2_{\rm gal}}\delta\varepsilon_{\rm PSF} + \frac{\delta(R^2_{\rm PSF})}{R^2_{\rm gal}}\varepsilon_{\rm PSF}\right\}$$

# Correcting the PSF

This result can be expressed in the familiar terms for a shear measurement error from the Shear TEsting Programme (STEP; Heymans et al. 2006; Massey et al. 2007b).

$$\widehat{\boldsymbol{\gamma}} = (1 + m)\boldsymbol{\gamma} + \boldsymbol{c} \tag{14}$$

where, dividing (13) by the shear polarizability,

$$\boldsymbol{c} = -\left(P_{\rm sh}\right)^{-1} \left\{ \frac{R^2_{\rm PSF}}{R^2_{\rm gal}} \boldsymbol{\delta\varepsilon}_{\rm PSF} + \frac{\delta(R^2_{\rm PSF})}{R^2_{\rm gal}} \boldsymbol{\varepsilon}_{\rm PSF} \right\} \tag{15}$$

$$m = \frac{\delta(R^2_{\rm PSF})}{R^2_{\rm gal}}. \tag{16}$$

# Finding the stars

The first step in the correction for the PSF is to identify a suitable sample of stars

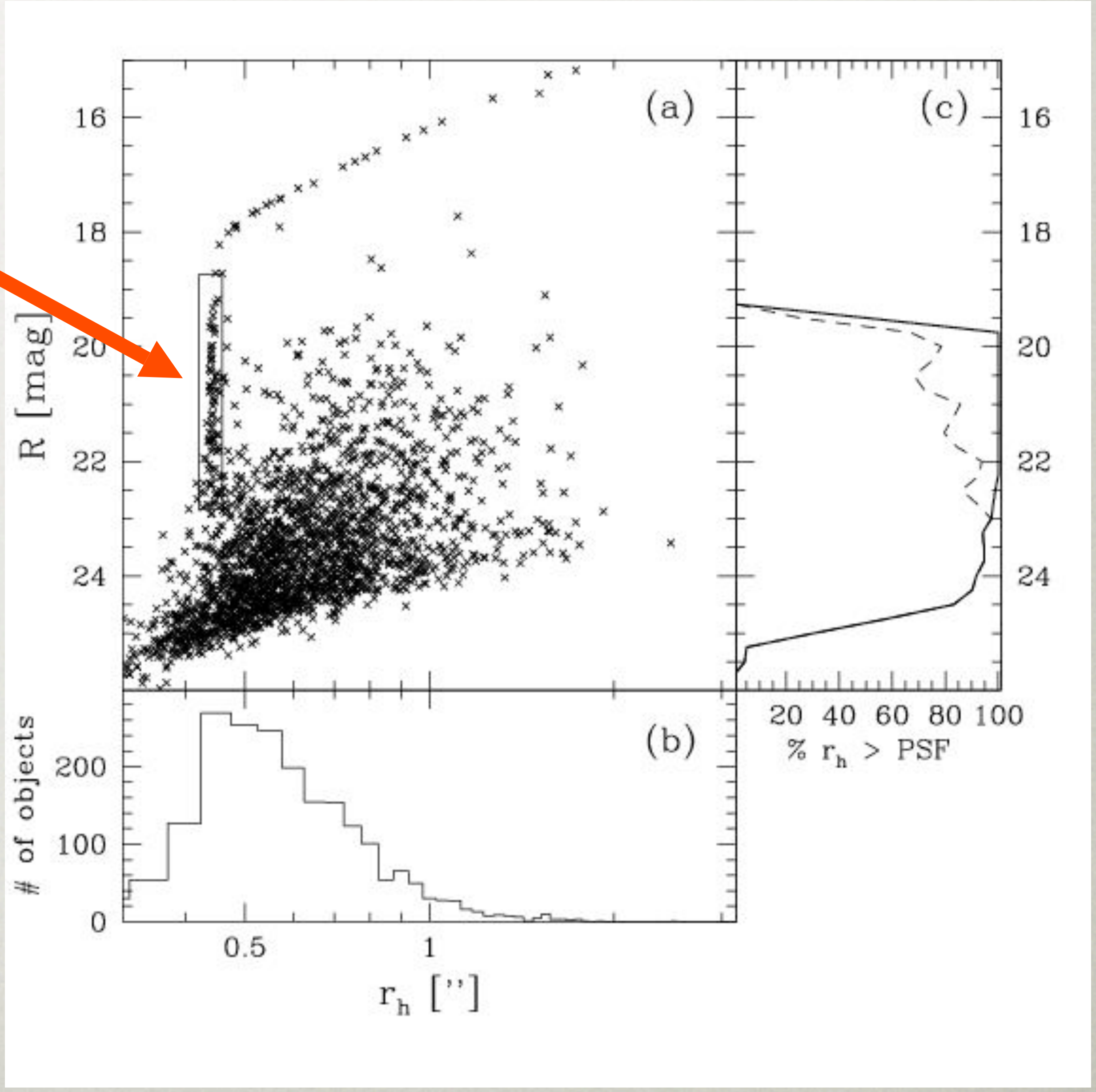

# The PSF

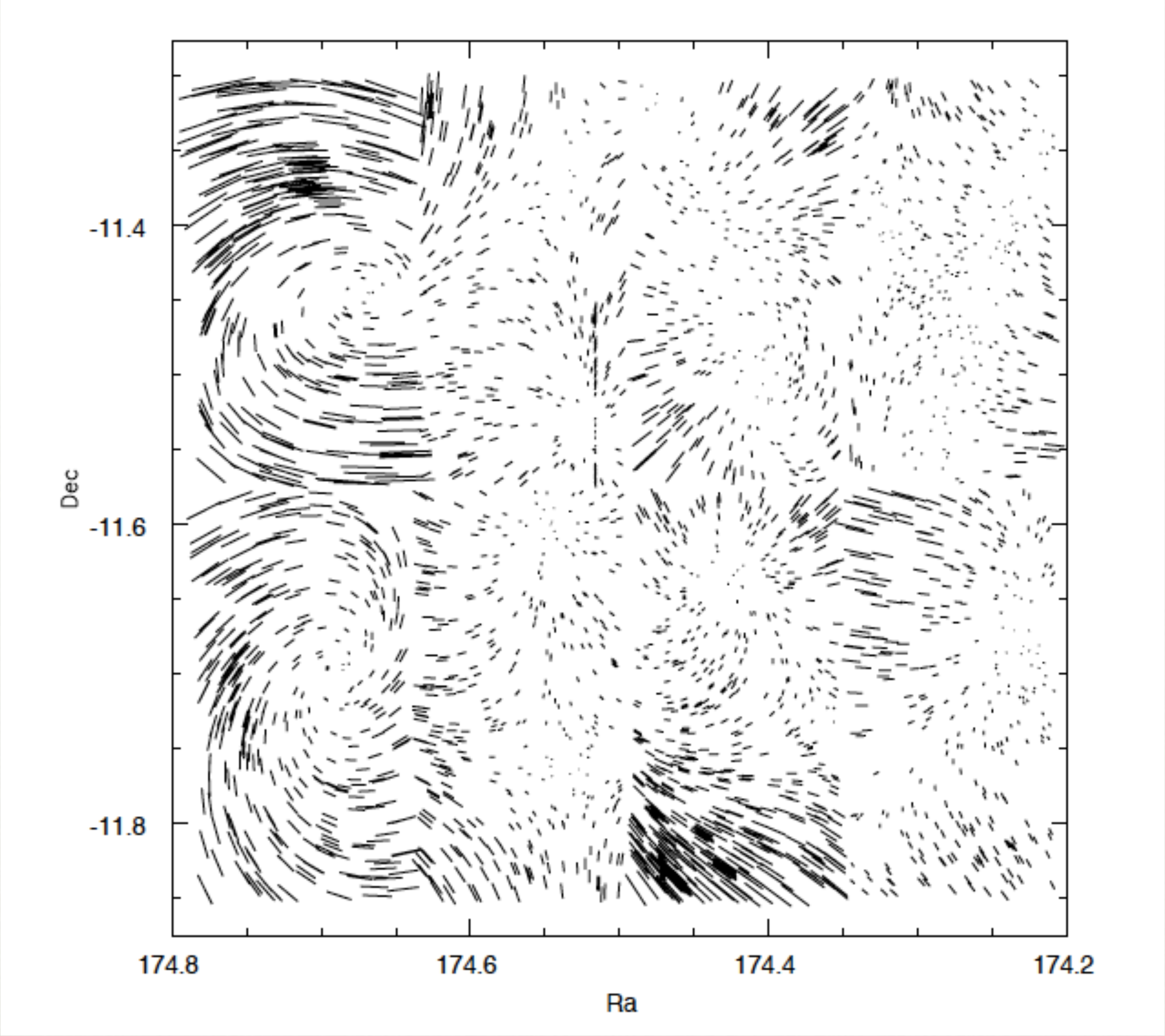


PSF anisotropy pattern for the WFI on the ESO 2.2m

# The PSF

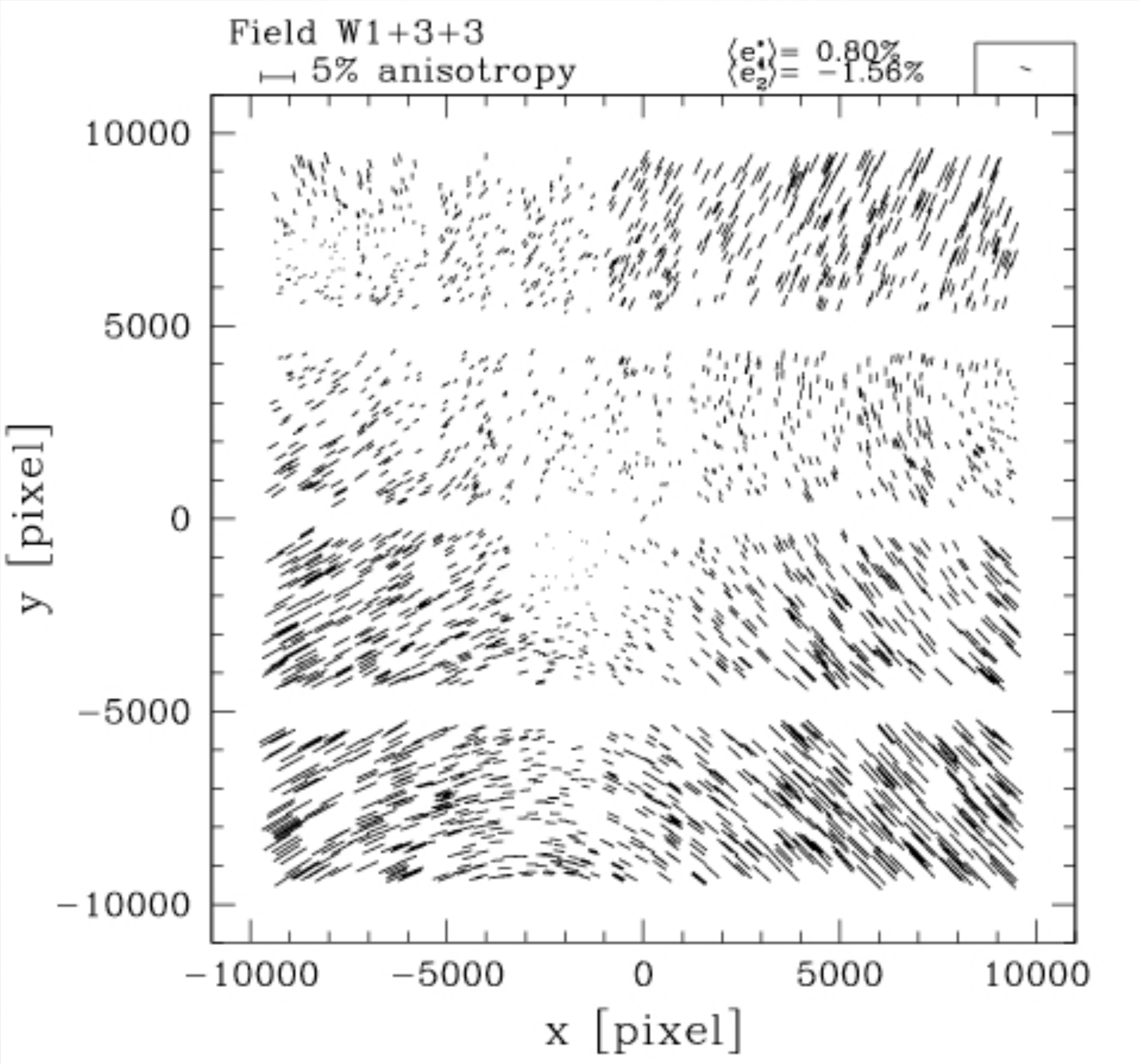


PSF anisotropy pattern for MegaCam on CFHT

# The PSF

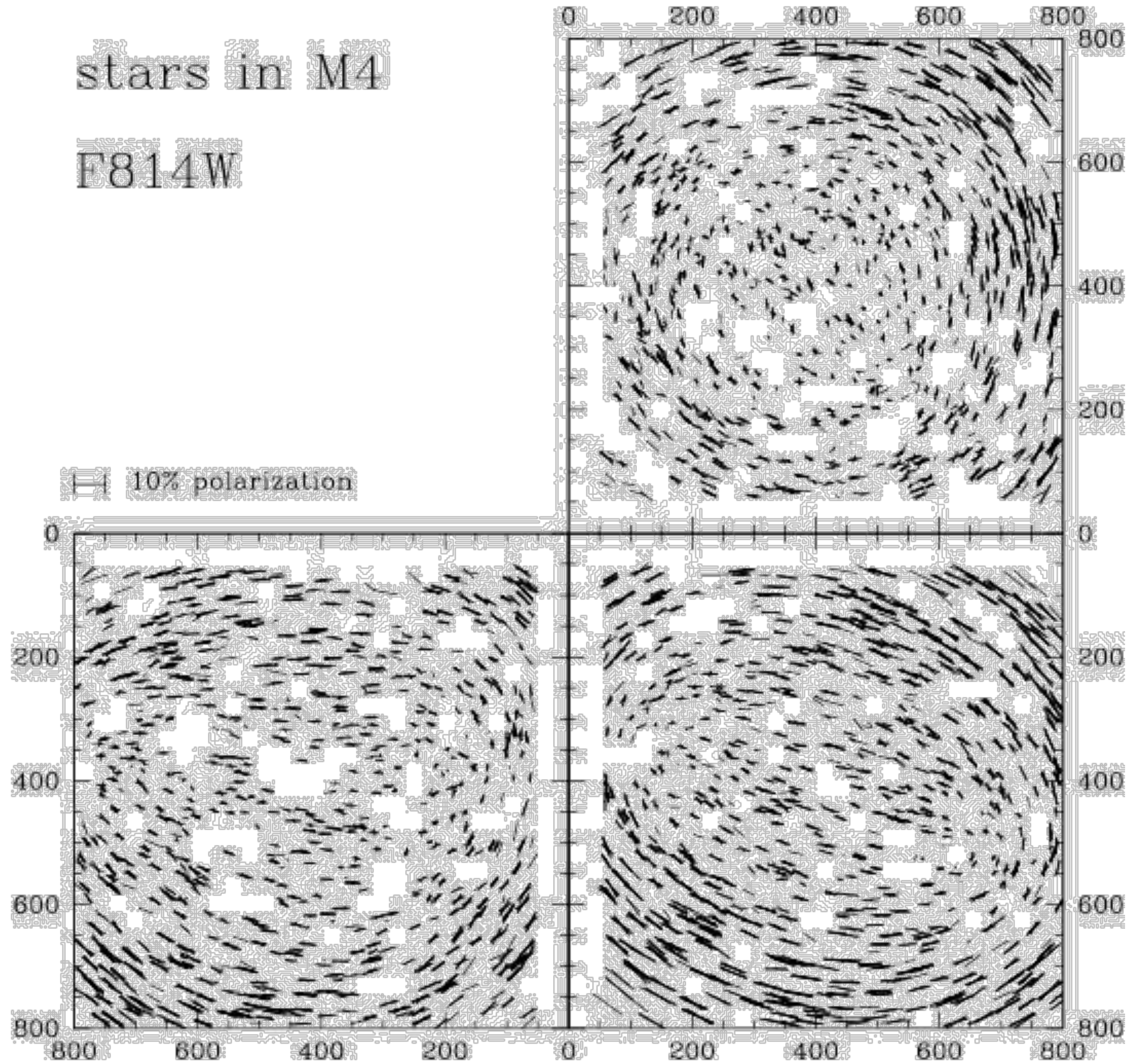


PSF anisotropy pattern for WFPC2 on HST

# PSF model

The PSF typically varies relatively smoothly, and one fits a parametric model to the measurements

A typical approach is to fit a low (2nd) order polynomial to the stars on each chip. However, near masked areas and chip edges the fit is poorly constrained. This can lead to overfitting.

A PCA analysis can reduce the number of fitted parameters, while effectively increasing the resolution of the model.

# Multiple exposures

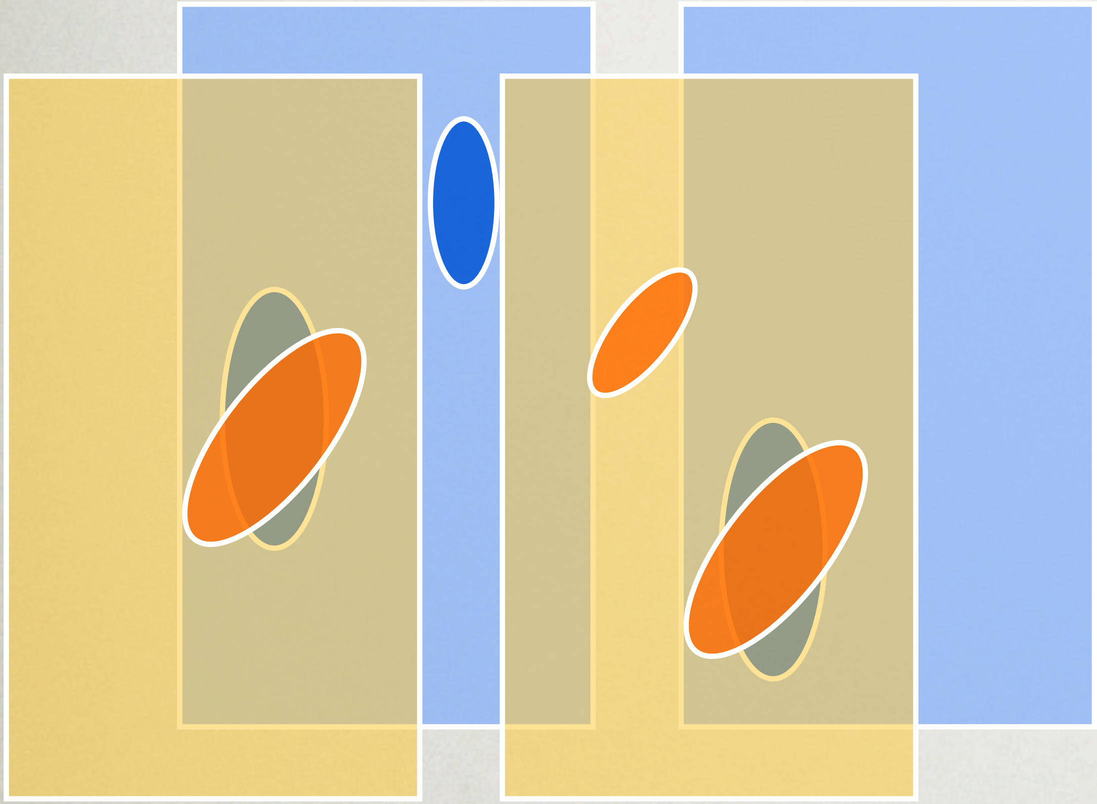

This leads to complicated PSF that vary across the image.

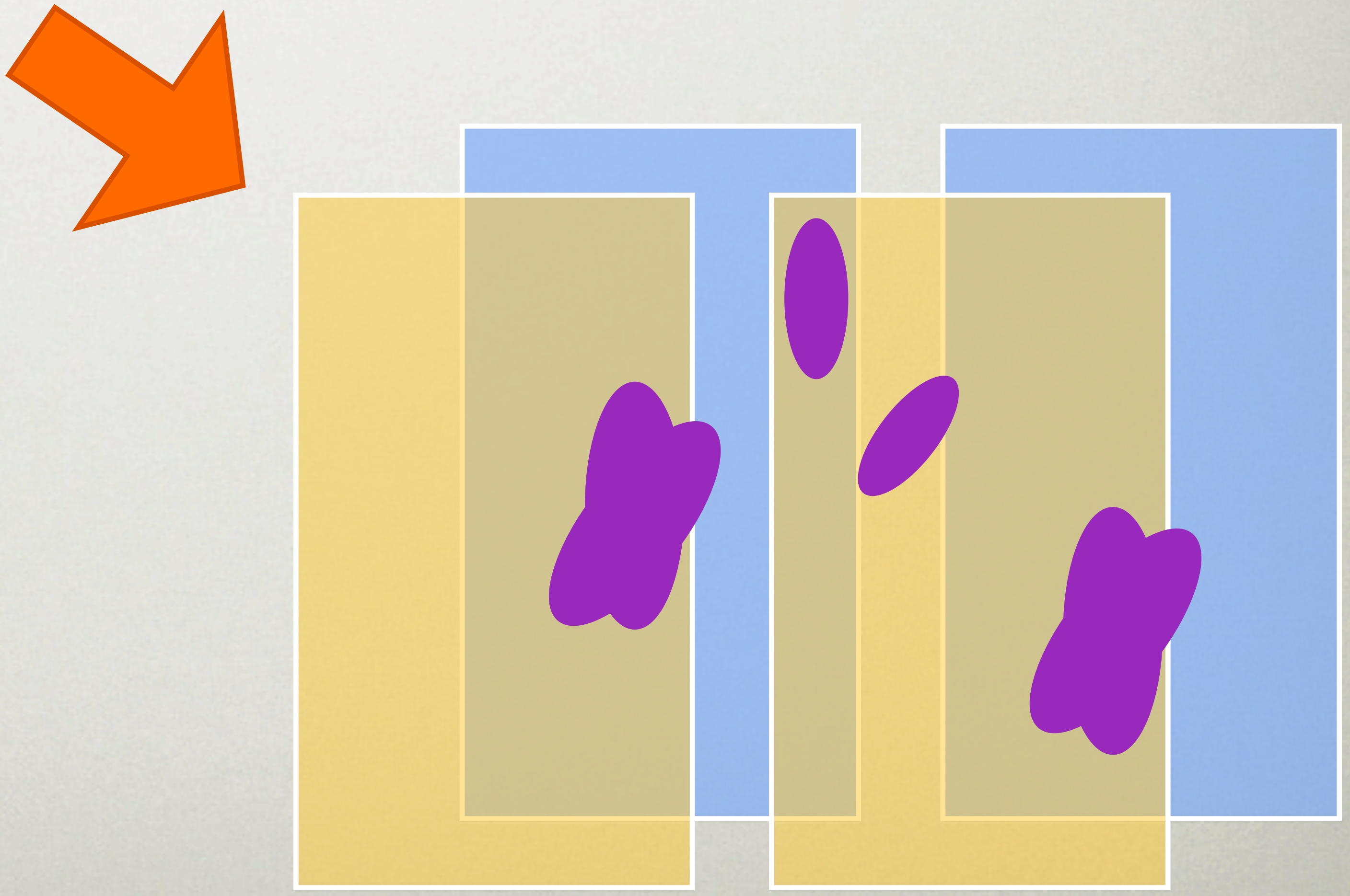

Observing conditions change between exposures

# Multiple exposures

Solutions:

Use a method that can operate on individual exposures: fit a single model, but with PSFs matched to each exposure.

Homogenize the PSF of images before stacking by convolving with an appropriate kernel. Need to keep track of modified noise properties.

# Correcting the PSF

There are two concerns with PSF correction:

- is the model for the PSF correct?
- **is the correction itself adequate?**

# Testing the results

The lensing signal is very small and the shape measurement of an individual galaxy cannot tell us whether the measurement was unbiased….

How can we test that everything worked well?

We have two (complementary) options:

- ❑ *Tests based on simulated data*
- ❑ *Tests based on real data*

# Testing the results

Weak lensing is rather unique in the sense that we can study systematics very well.

data

Several diagnostic tools can be used. However, knowing systematics are present doesn't mean we know how to deal with them…

simulation

But we can readily simulate weak lensing surveys. A number of challenges are aiming to improve our techniques this way. But we still need to check the real data…

# Simulating data

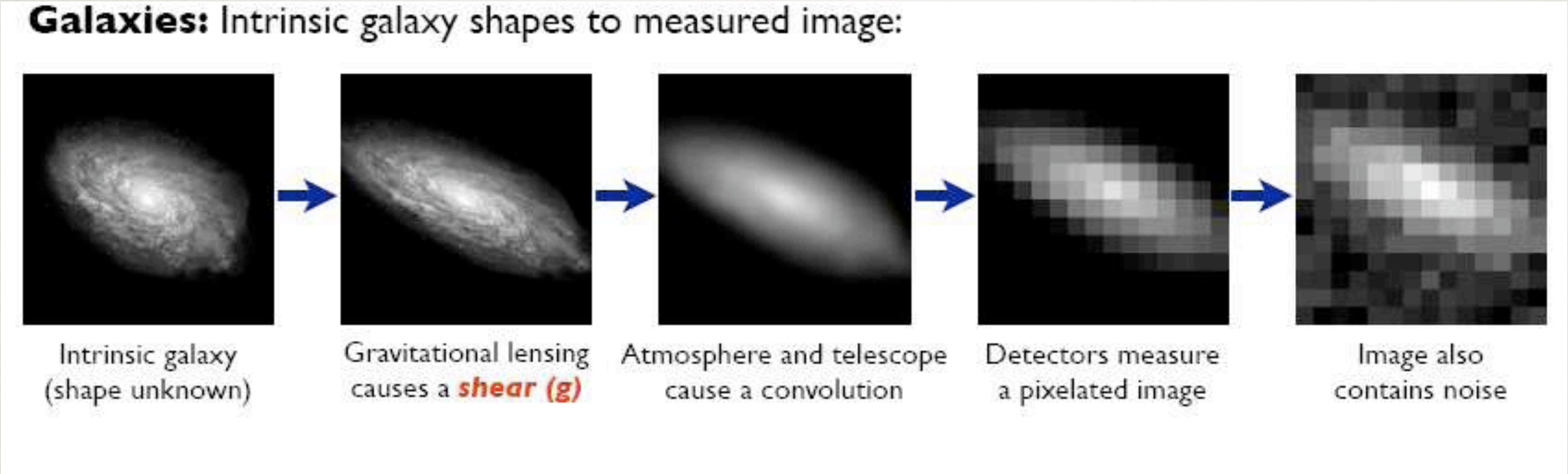


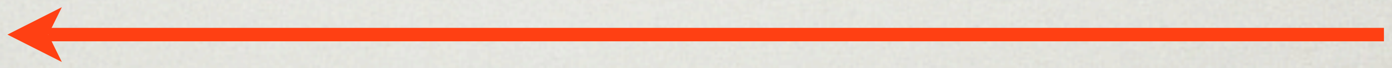

How accurate can we do the inversion?

# Correction methods

Much work is devoted to improve correction itself and this very much a work in progress. Various methods and how they perform have been examined in the STEP1, STEP2, GREAT'08 and GREAT'10 papers.

The focus of development are techniques to fit PSF-convolved models to the observed galaxy images.

The problem is what models to use (minimize the number of parameters to be fitted) and how to do this fast.

# Challenges

Shear TEsting Programme (STEP):

STEP1: Heymans et al. 2006, MNRAS, 368, 1323
STEP2: Massey et al. 2007, MNRAS, 376, 13

Gravitational Lensing Accuracy Testing (GREAT):

GREAT'08: Bridle et al. 2010, MNRAS, 405, 2044
GREAT'10: Kitching et al. 2012, MNRAS, 423, 3163

# STEP1

$$\gamma_1 - \gamma_1^{\rm true} = m\gamma_1^{\rm true} + c_1$$

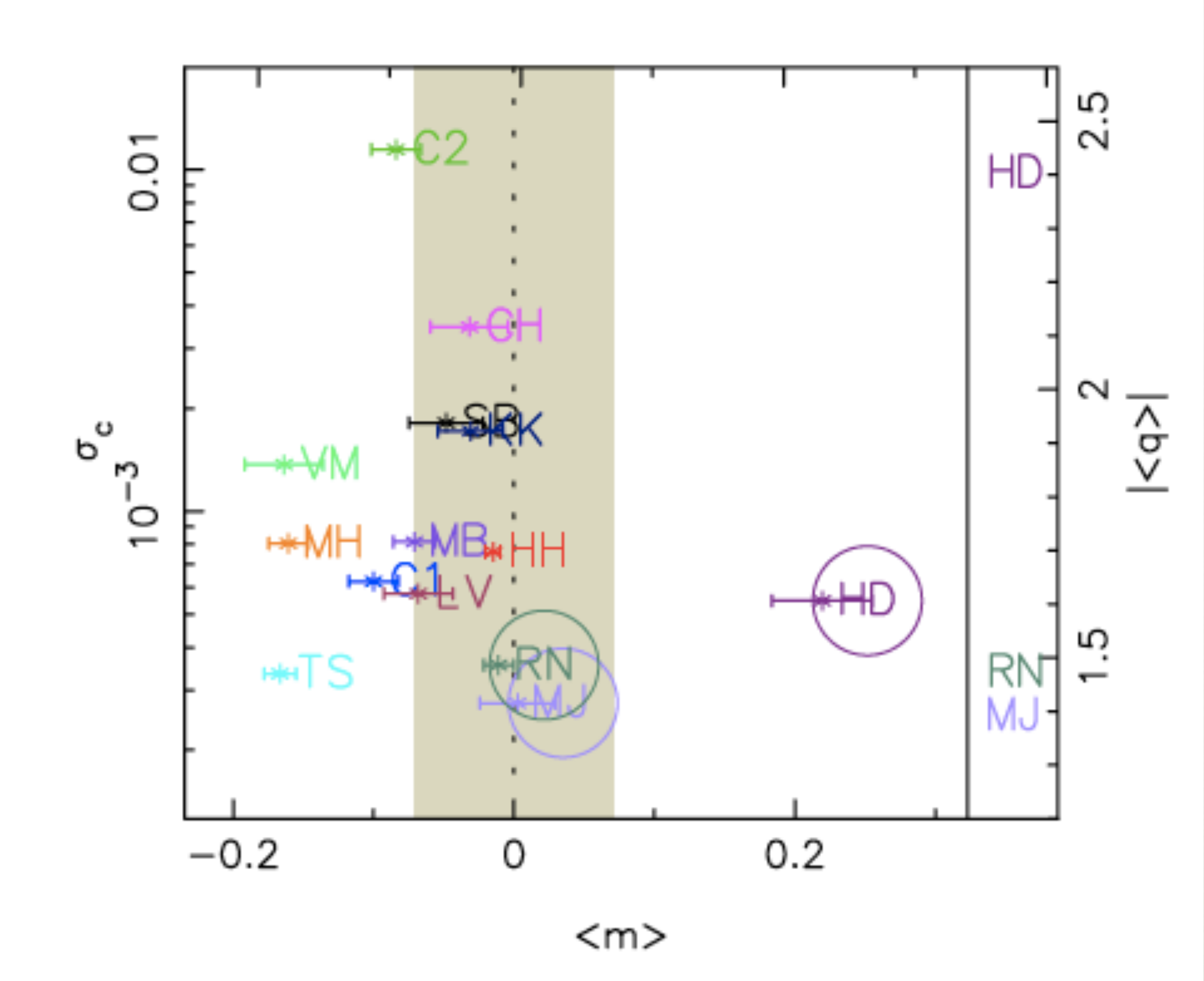

# GREAT'10

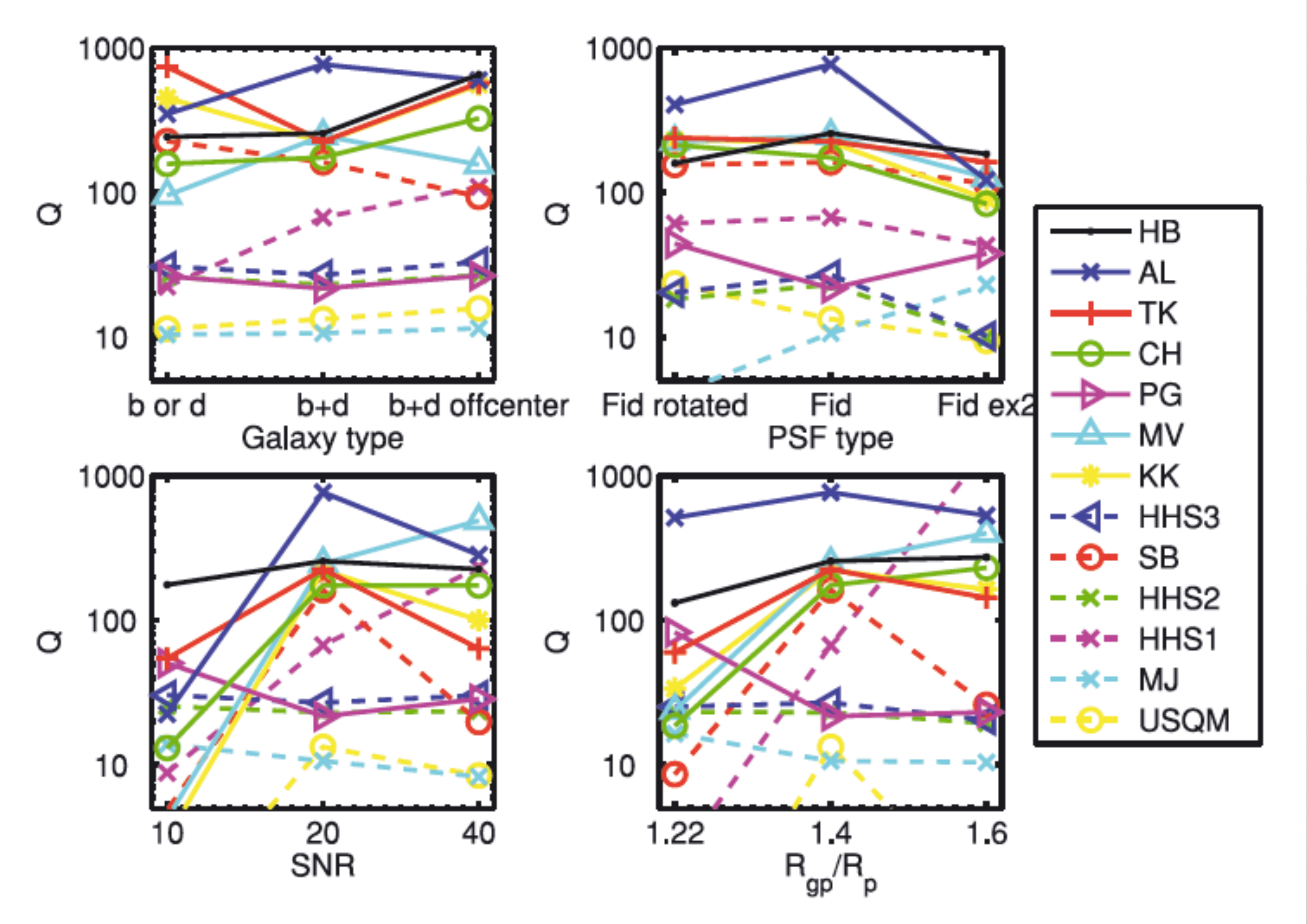

1000
100
10
Q
b or d
b+d
b+d offcenter
Galaxy type
Fid rotated
Fid
Fid ex2
PSF type
10
20
40
SNR
1.22
1.4
1.6
$R_{gp}/R_p$
HB
AL
TK
CH
PG
MV
KK
HHS3
SB
HHS2
HHS1
MJ
USQM

# Simulated data

Image simulations should match the observed properties of galaxies and the PSF (Miller et al., in prep.)

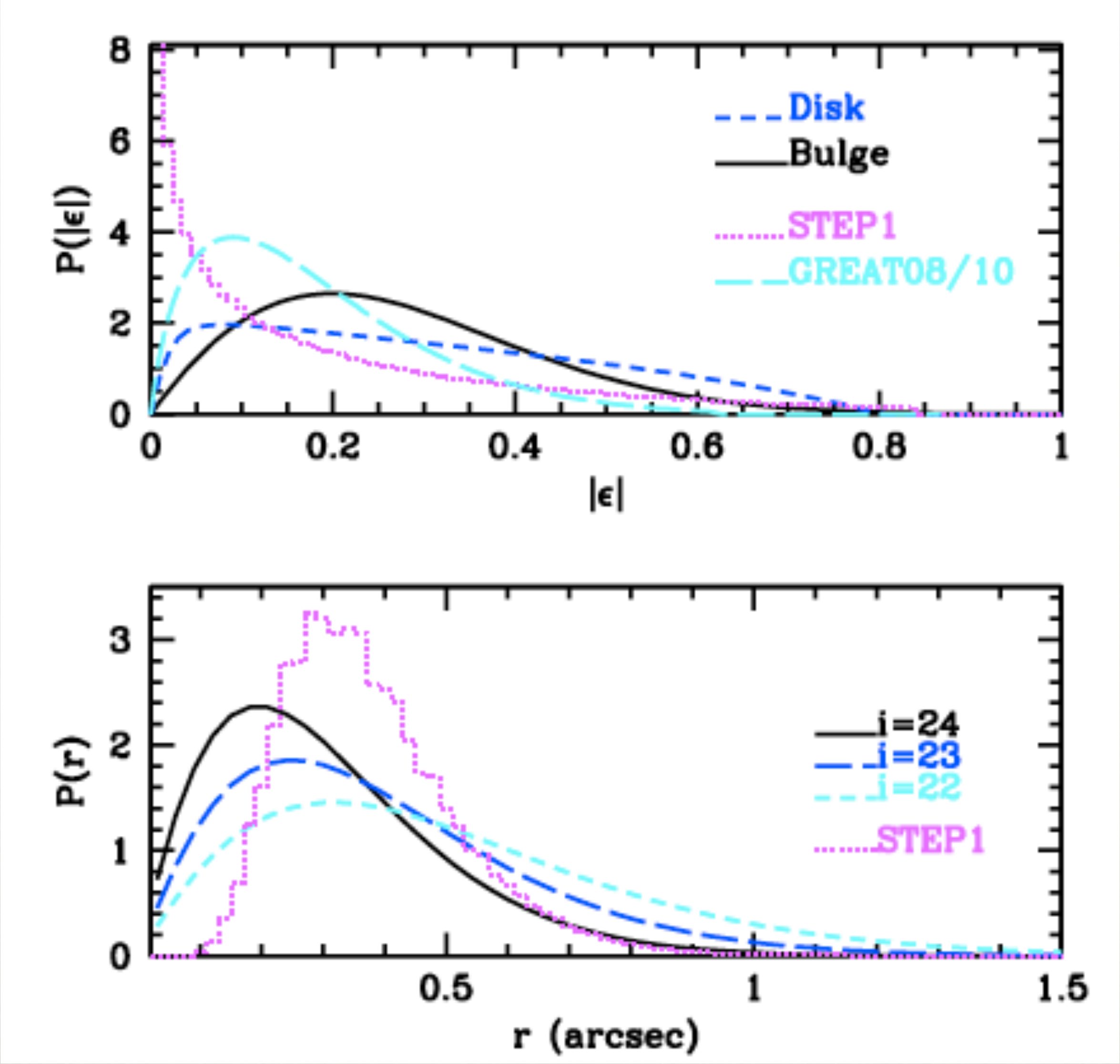

# Observational tests

The star-galaxy correlation function provides a *cosmology independent* way to assess the level and significance of PSF-related systematics

*Star-galaxy correlation:*

$$\xi_{\rm sys}(\theta) = \frac{\langle e^\star(x)\gamma(x+\theta)\rangle^2}{\langle e^\star(x)e^\star(x+\theta)\rangle}$$

# Observational tests

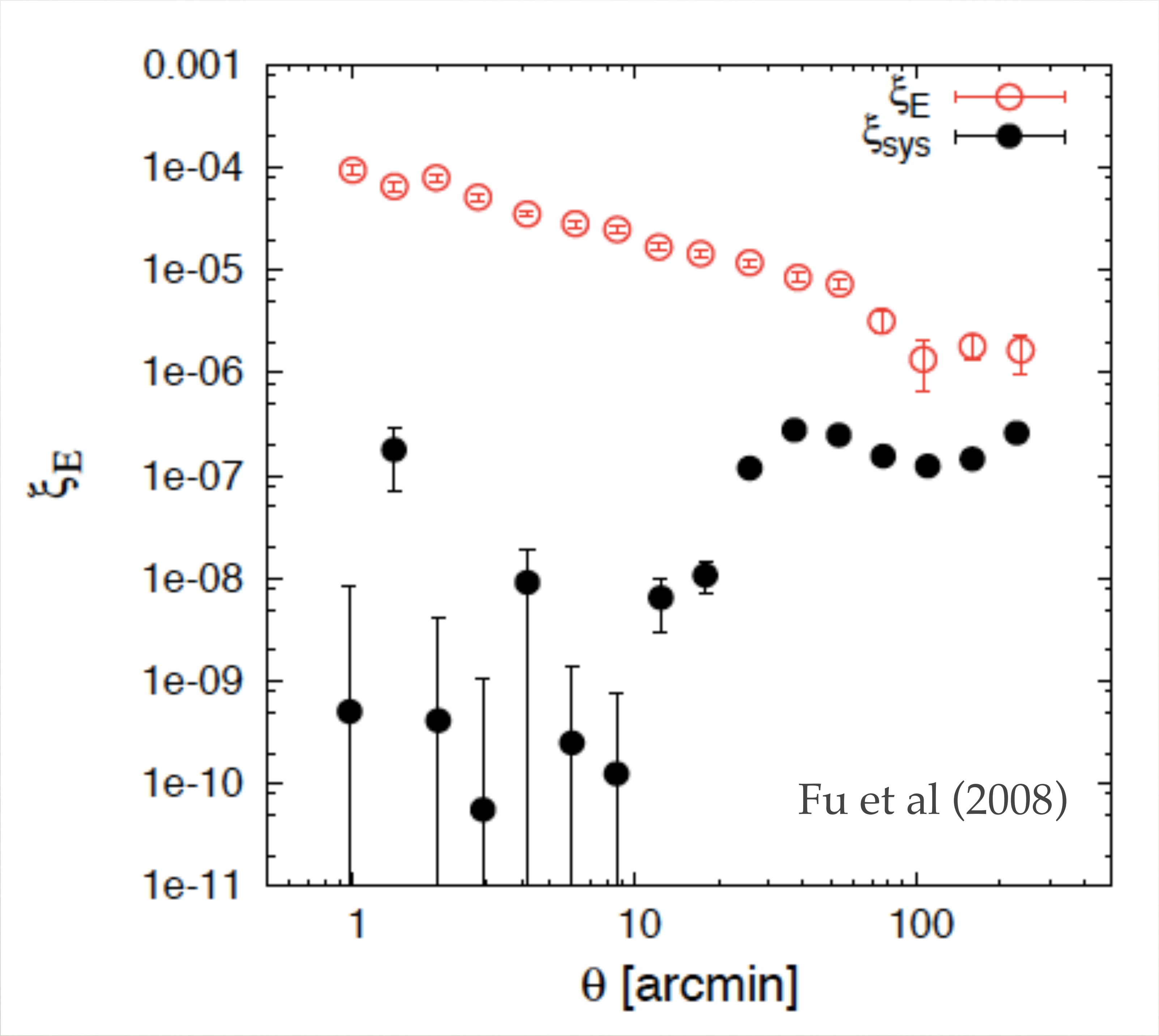

# Observational tests

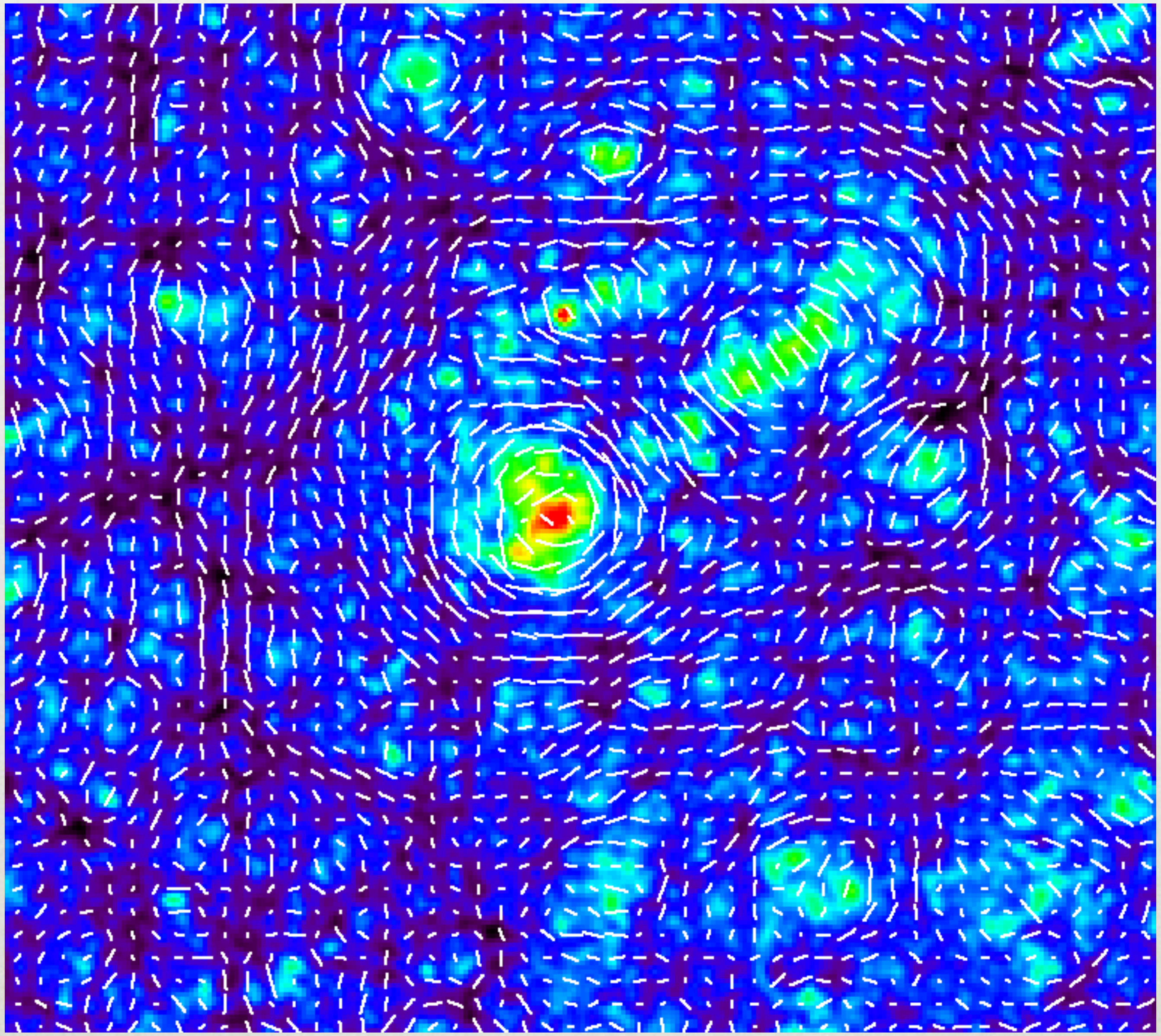

What can the shear itself tell us?

# Observational tests

See Schneider, van Waerbeke & Mellier (2002) for more details.

The shear field is a two dimensional quantity, whereas the projected density field of the matter is a scalar field.

If we write $\gamma(\boldsymbol{\theta}) = \gamma_1(\boldsymbol{\theta}) + \mathrm{i}\gamma_2(\boldsymbol{\theta})$

then
$$\gamma(\boldsymbol{\theta}) = \frac{1}{\pi} \int_{\mathbb{R}^2} \mathrm{d}^2\theta' \, \mathcal{D}(\boldsymbol{\theta} - \boldsymbol{\theta}') \kappa(\boldsymbol{\theta}') \, ,$$

where
$$\mathcal{D}(\boldsymbol{\theta}) = \frac{\theta_2^2 - \theta_1^2 - 2\mathrm{i}\theta_1\theta_2}{|\boldsymbol{\theta}|^4} \, ;$$

# Observational tests

Kaiser & Squires (1993):

$$\kappa^{\mathrm{E}}(\boldsymbol{\theta}) + \mathrm{i}\kappa^{\mathrm{B}}(\boldsymbol{\theta}) = \frac{1}{\pi} \int_{\mathbb{R}^2} \mathrm{d}^2\theta' \mathcal{D}^*(\boldsymbol{\theta} - \boldsymbol{\theta}')\,\gamma(\boldsymbol{\theta}'),$$

The complex shear $\gamma = \gamma_1 + \mathrm{i}\gamma_2$ is obtained from the potential $\psi$ by $\gamma = D\psi$, where the differential operator $D = (\partial_{11} - \partial_{22})/2 + \mathrm{i}\partial_{12}$; hence,

$$\gamma = \left[\frac{1}{2}\left(\psi^{\mathrm{E}}_{,11} - \psi^{\mathrm{E}}_{,22}\right) - \psi^{\mathrm{B}}_{,12}\right] + \mathrm{i}\left[\psi^{\mathrm{E}}_{,12} + \frac{1}{2}\left(\psi^{\mathrm{B}}_{,11} - \psi^{\mathrm{B}}_{,22}\right)\right].$$

# Observational tests

Indeed, the shear field can be decomposed into E/B-modes, $\gamma = \gamma^{\rm E} + {\rm i}\gamma^{\rm B}$, with

$$\gamma^{\rm E} = \frac{\mathcal{D}}{\pi} * \mathcal{R}{\rm e}\left[\frac{\mathcal{D}^*}{\pi} * \gamma\right],$$

$$\gamma^{\rm B} = \frac{\mathcal{D}}{\pi} * \mathcal{I}{\rm m}\left[\frac{\mathcal{D}^*}{\pi} * \gamma\right],$$

This is now referred to as E-B mode decomposition

# Observational tests

E-mode (curl-free)

B-mode (curl)

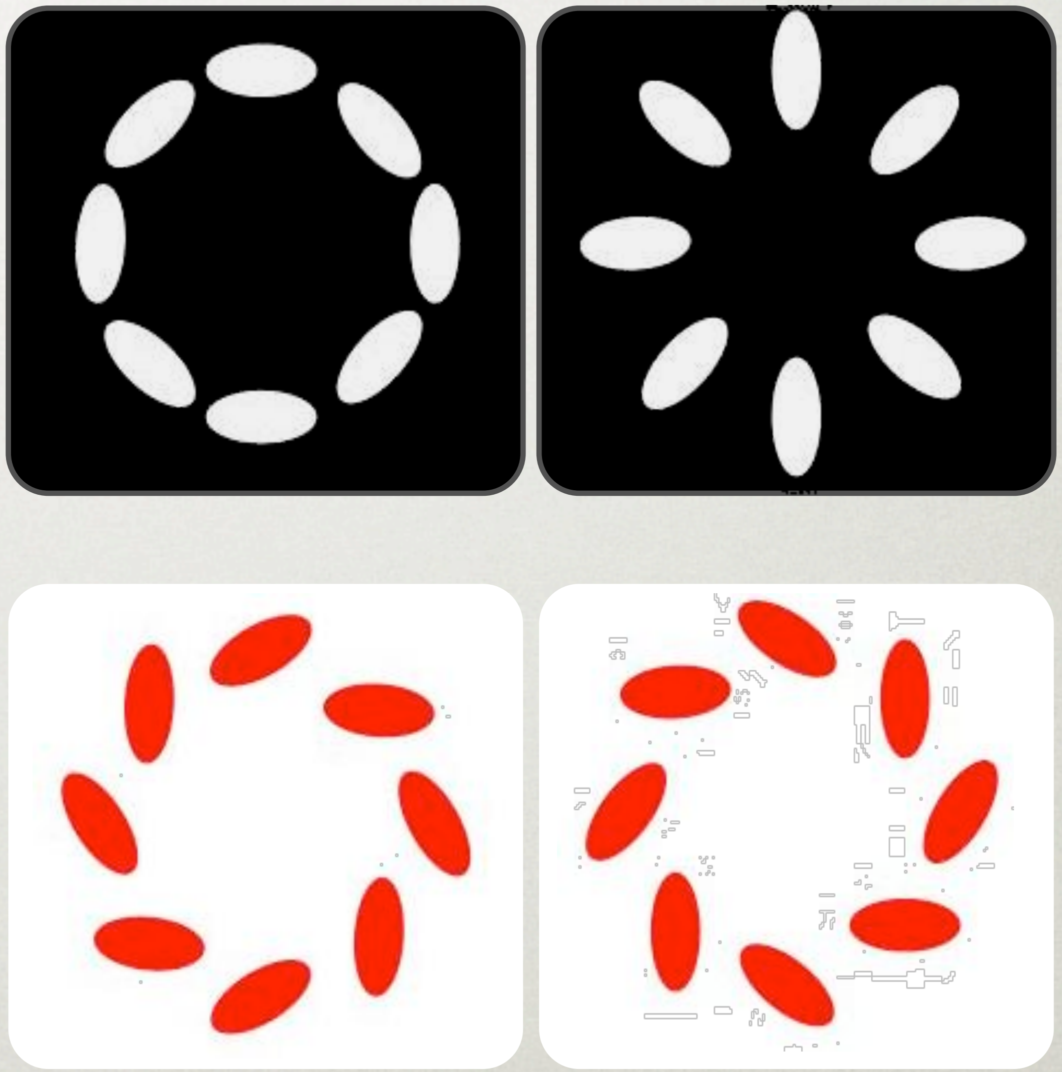

# Observational tests

defining the tangential and cross-component of the shear at position $\boldsymbol{\vartheta}$ for this pair as

$$\gamma_{\rm t} = -\mathcal{R}{\rm e}\left(\gamma\, {\rm e}^{-2{\rm i}\varphi}\right), \quad \gamma_\times = -\mathcal{I}{\rm m}\left(\gamma\, {\rm e}^{-2{\rm i}\varphi}\right), \tag{13}$$

respectively, where $\varphi$ is the polar angle of the separation vector $\boldsymbol{\theta}$. Then, the shear correlation functions are defined as

$$\begin{aligned} \xi_+(\theta) &= \langle\gamma_{\rm t}\gamma_{\rm t}\rangle + \langle\gamma_\times\gamma_\times\rangle(\theta), \\ \xi_-(\theta) &= \langle\gamma_{\rm t}\gamma_{\rm t}\rangle - \langle\gamma_\times\gamma_\times\rangle(\theta), \\ \xi_\times(\theta) &= \langle\gamma_{\rm t}\gamma_\times\rangle(\theta). \end{aligned} \tag{14}$$

# Observational tests

One very convenient way to separate E- and B-modes is provided by the aperture mass: defining the tangential and cross component of the shear relative to the center of a circular aperture of angular radius $\theta$, and defining

$$M_{\mathrm{ap}}(\theta) = \int \mathrm{d}^2\vartheta\, Q(|\vartheta|)\, \gamma_{\mathrm{t}}(\boldsymbol{\vartheta}),$$

$$M_{\perp}(\theta) = \int \mathrm{d}^2\vartheta\, Q(|\vartheta|)\, \gamma_{\times}(\boldsymbol{\vartheta}), \quad (27)$$

Here $Q$ is a compensated filter (Schneider et al. 1998)

# Observational tests

We can look at the ellipticity correlation functions of the stars before and after correction. This tests whether we used the correct model.

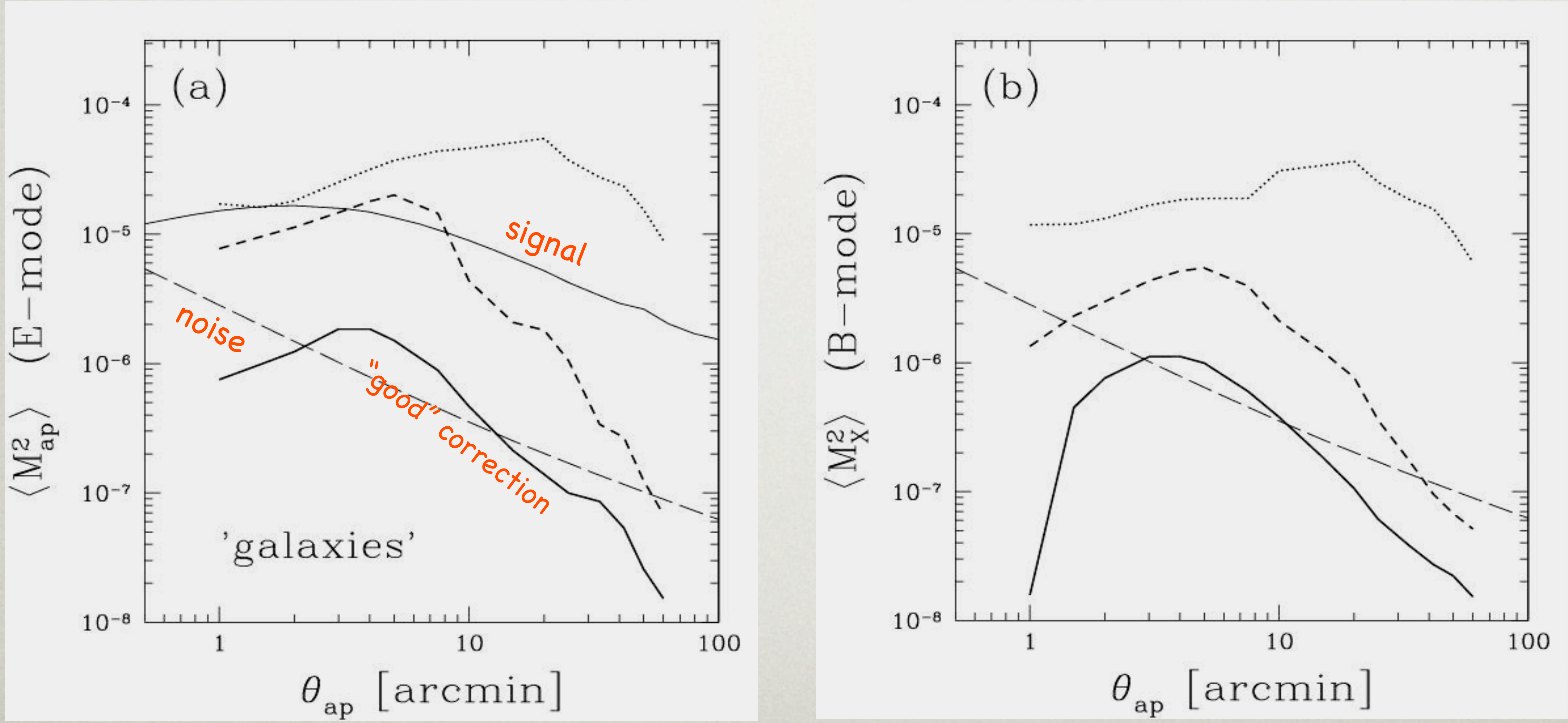


Hoekstra (2003), Based on EXPLORE2 data

# Observational tests

The B-mode of the cosmic shear signal is another diagnostic. If it is non-zero the correction itself is flawed.

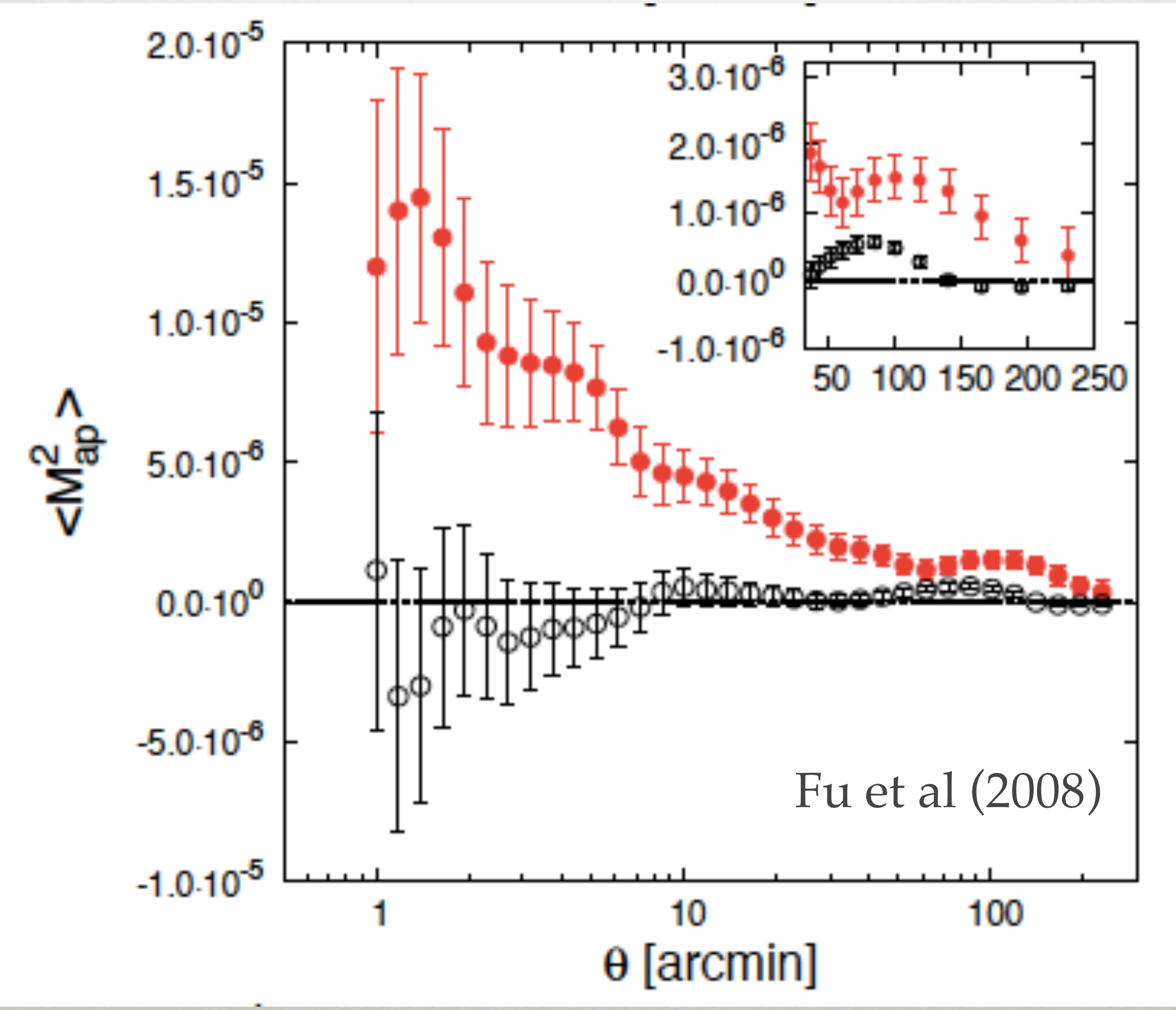

# Conclusions

In theory measuring shapes is easy, but in practice it is much harder!

The study of shape measurement techniques is an area of active research and there are still many open questions. Future projects require a significant improvement over current technique.